sharing drive innovation

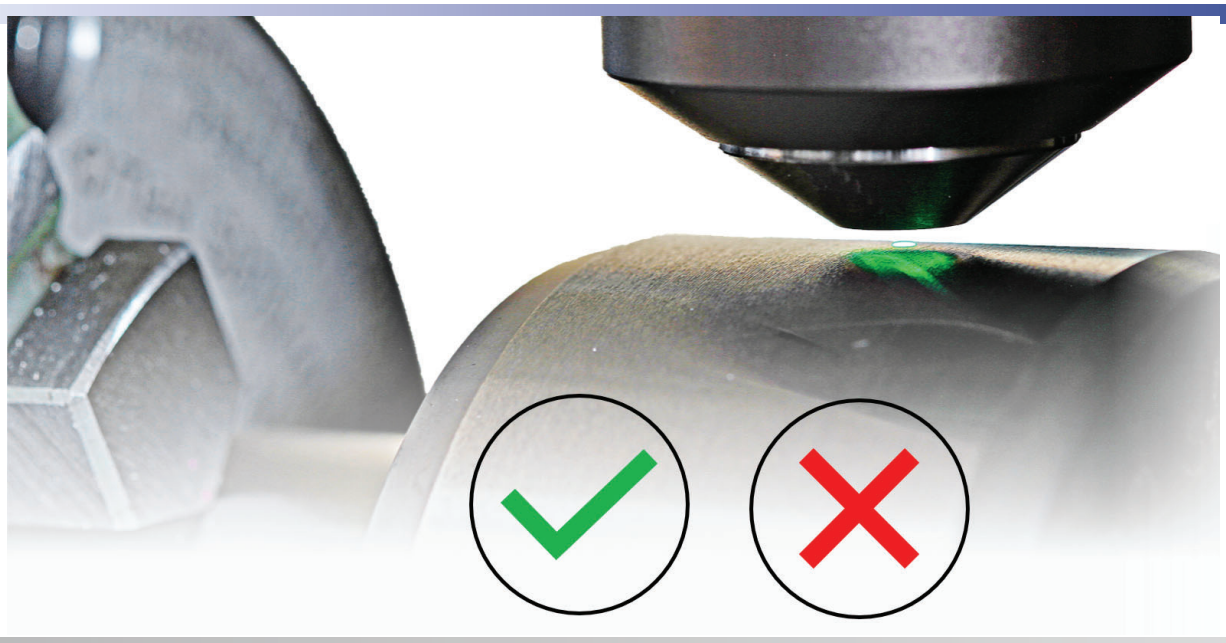

FVA-Guideline

SURFACES/LEAD - SHAFT SEALS

2026 Edition V3

Release Date: 24.04.2026

FVA 975 I	**GUIDELINE:** **SURFACES/LEAD – SHAFT SEALS** **V3**	sharing drive innovation

FVA Guideline Surfaces/Lead - Shaft Seals

Topic: Development of an FVA Guideline with surface and lead requirements for seal countersurfaces for shaft seals

Short Summary:

The FVA Guideline "Surfaces/Lead - Shaft Seals" presents a compact summary of the current state of research on the surface condition of plunge-ground seal countersurfaces of rotary shaft seals. The guideline focuses on the presentation of methods for measuring, characterizing and evaluating lead. The term “lead” refers to all types of microscopic and macroscopic surface structures on the shaft surface that actively pump fluid in the sealing contact when the shaft rotates and can result in failure of the sealing system.

The FVA guideline serves as a comprehensive guide for analyzing the surface conditions of a seal countersurfaces, enabling companies to correctly assess seal countersurfaces independently and in cooperation with suppliers and customers without having to rely on external expertise.

Scope of application: Seal countersurfaces for rotary shaft seals in the mechanical engineering/drive technology sector in accordance with DIN 3760/3761, which are manufactured using the external cylindrical grinding process in a plunging process.

Table of Contents

1 Introduction

The surface condition of the seal countersurface of rotary shaft seals has a significant influence on the sealing function of a rotary shaft sealing system, see Figure 1. The machining process, surface deviations (form, waviness and roughness), surface imperfections (scratches, dents, rust) of the shaft surface and lead must be considered. Each of these issues on its own can have a detrimental effect on a sealing system, causing leakage or system failure, which ultimately affects the reliability of products.

The aim of this guideline is to summarize the current state of knowledge on the subject of 'lead on the seal countersurface' and to establish a generally applicable terminology by defining terms. In addition, currently available measuring methods and procedures are presented and recommendations and specifications are provided for the design of reliable rotary shaft sealing systems. By establishing a standardized procedure for the measurement, evaluation and assessment of seal countersurfaces, a basis for the quality assurance of the corresponding products is to be created.

Figure 1 shows the contents of the guideline, focusing on the topic of lead. The guideline also briefly explains other relevant surface properties of the seal countersurface that are already contained in standards and guidelines.

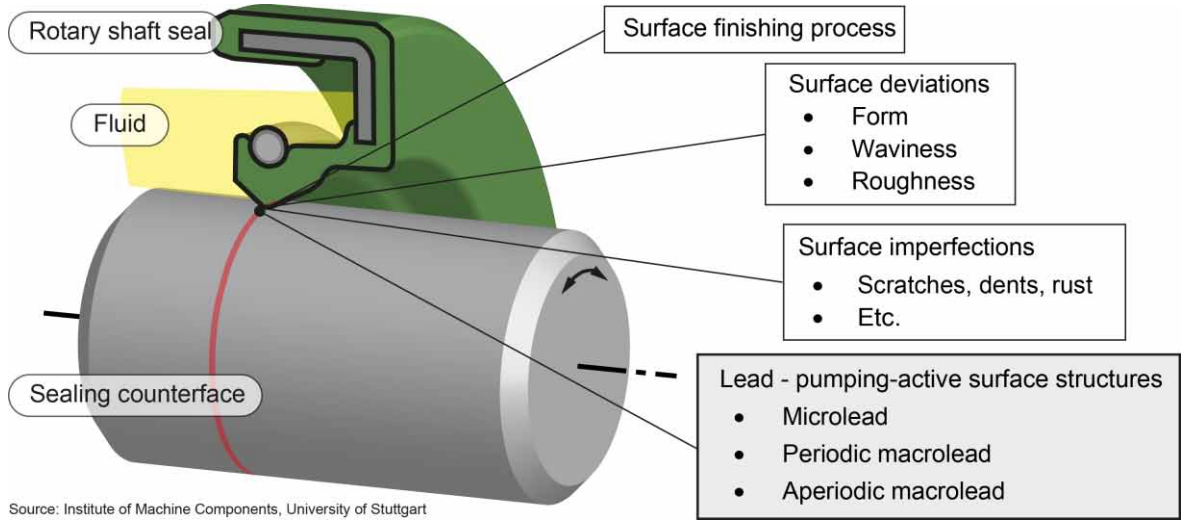

Figure 1: Contents of FVA Guideline 975 I 'Surfaces/Lead - Shaft seals'

2 Scope of Application

The FVA Guideline 'Surfaces/lead - shaft seals' applies to seal countersurfaces for rotary shaft seals in the field of mechanical engineering/drive technology in accordance with DIN 3760/3761 [1, 2], which are manufactured using the cylindrical plunge grinding machining process. All specified tolerance ranges are recommendations and are not to be understood as absolutely strict limit values. Limits must generally be determined or harmonized individually and on an application-specific basis, as these are highly dependent on the application.

3 Normative References

DIN 3760:1996 [1]	Rotary shaft lip type seals
DIN 3761:1983 [2]	Rotary shaft lip type seals for automobiles
DIN 4760: 1982 [3]	Formdeviation
DIN EN ISO 21920-1-3 [4–6]	Surface texture: Profile
DIN EN ISO 25178-1-3 [7–9]	Surface texture: Areal
DIN EN ISO 8785 [10]	Surface imperfections
DIN EN ISO 3274: 1998 [11]	Surface texture: Profile method
DIN EN ISO 16610-1 [12]	Filtration – Overview and basic concepts
MBN 31007-7: 2008 [13]	Surface texture: Measurement and evaluation method for the assessment of leadreduced dynamic sealing surfaces
VDA 2006 [14]	Surface texture: Rules and procedures for the assessment of surface texture
VDA 2007 [15]	Surface texture: Definitions and parameters of the dominant waviness
RMA OS-1-1 [16]	Shaft finish requirements for radial lip seals

4 Terms

Seal Countersurface

The seal countersurface is defined as the area of the shaft surface that is in tribological contact with the sealing edge of the rotary shaft seal.

Surface Finishing Process

The surface finishing process is the final production stage in the manufacturing process of the seal countersurface. The objective of this stage is to create specific shapes (such as roundness and straightness) and surface characteristics (such as roughness and lead-free) on the shaft surface. This is typically achieved through the removal of material.

Lead

Lead summarizes the surface structures of the seal countersurface that direct the fluid flow in the sealing gap in an axial direction during dynamic operation of the rotary shaft sealing. This action affects the tribological conditions in the sealing contact. The presence of lead can result in leakage and failure of the sealing system. A number of different lead categories exist that may even occur in superposition on the seal countersurface.

Microlead

Microlead describes pumping-active grinding grooves that are stochastically distributed on the seal countersurface. They are created by the grain engagement of individual abrasive grains during the grinding process and form the fine structure of the seal countersurface.

Macrolead

Macrolead describes pumping-active periodic or aperiodic structures on the seal countersurface. These structures are created by a kinematic replication process of the grinding wheel contour onto the shaft surface during the grinding process and form the coarse structure of the seal countersurface.

Surface Imperfections

Surface imperfections are defined according to DIN EN ISO 8785 [10] and include, for example, scratches, dents, burrs or rust. Surface imperfections may impact the functionality of a rotary shaft seal in several ways. Such effects include, for example, significant increase in the wear of the sealing edge or the axial pumping of oil through the sealing gap. This may result in both dynamic and static leakage.

Surface Deviations

Surface deviations according to DIN 4760 [3] describe and classify the deviations of the actual surface from the nominal surface.

Lead Measurement

Lead measurement includes methods for measuring and evaluating lead on seal countersurfaces, further subdivided into microlead and macrolead measurement.

Structure-based Lead Analysis

Structure-based analysis methods identify, locate, and analyze individual structural elements (grinding grooves and grinding structures) in the surface measurement data and evaluate them statistically in total. The structure-based lead analysis is based on 3D topography data, which are usually captured with optical surface measuring devices.

Qualitative Testing Methods

Qualitative testing methods are methods for describing and evaluating properties or characteristics of a phenomenon without quantitative values. The result is a binary decision characteristic (yes/no).

Quantitative Measuring Methods

Quantitative measuring methods are methods for the precise numerical measurement of sizes, quantities, or properties of a phenomenon. An example of this is the metrological determination of lead depth.

Tactile Surface Measuring Methods

Tactile surface measuring methods measure the surface according to the profile method, which is standardized in DIN EN ISO 3274 [11]. The form, waviness, and roughness of the shaft surface are determined from surface profiles using tactile surface measuring methods.

Optical Surface Measuring Methods

Optical surface measuring methods are measuring techniques that use various properties of light and optical sensors to generate three-dimensional topographies of the shaft surface.

Measurement Grid

The measurement grid defines the arrangement of measuring field positions on the shaft surface and the measuring field sizes.

Wobble Compensation

A cylindrical component part (shaft), which is clamped at an angle in the chuck of a measuring device, performs a wobbling movement during rotation. This results in circumferential-dependent angular misalignments that are transferred to the measurement data and impact the accuracy of the analysis result. The so-called wobble compensation employs algorithms to correct these angular errors. However, certain conditions for the measurement grid are required for its implementation.

Surface Stitching

The assembly of the surface topographies of several overlapping measuring fields into a single large surface topography is called surface stitching.

5 Surface Characteristics of Seal Countersurfaces – Fundamentals

The surface characteristics of a seal countersurface significantly influence the tribological system "rotary shaft seal." A comprehensive summary of the current state of knowledge on rotary shaft seals and their functional mechanisms, such as the active sealing mechanism performed during dynamic operation, can be found in [17]. Below are important properties and the currently known influence mechanisms of the seal countersurface on the rotary shaft seal system, as well as other relevant points.

5.1 Surface Finishing Process

It is recommended to use cylindrical plunge grinding as the surface finishing process of the seal countersurface. Empirical tribological studies of the past decades have shown that the resulting surface structure provides optimal hydrodynamic properties for sealing with elastomer rotary shaft seals.

Alternative processes such as various turning or rolling processes can also be used for finishing the seal countersurface. However, compared to the cylindrical plunge grinding, these processes result in seal countersurfaces with poorer hydrodynamic properties, thereby limiting the possible operating conditions regarding maximum shaft circumferential speed and application temperature. Empirical testing is strongly recommended when using such alternative surface finishing processes.

5.2 Surface Deviations of the Seal Countersurface

According to DIN 4760 [3], the relevant surface deviations of the seal countersurface include deviations of the 1st order (form), 2nd order (waviness), and 3rd and 4th orders (roughness).

5.2.1 Form and Waviness of the Seal Countersurface

Deviations in form and waviness of the seal countersurface outside the tolerance range of common standards for rotary shaft seals (e.g., DIN 3761 [2]) are problematic. Due to the viscoelastic behavior of the material, the sealing edge of the rotary shaft seal may lose its ability to follow the relative radial movement of the shaft surface during dynamic operation. This can result in leakage.

5.2.2 Surface Roughness of the Seal Countersurface

The surface roughness of the seal countersurface affects the wear behavior of the components of the sealing system, as well as the active sealing mechanism and the tribological condition in the sealing contact. Reliable sealing function over an extended period requires adherence to a two-sided limited tolerance range of surface roughness. Too rough seal countersurfaces lead to increased wear of the sealing edge and consequently to leakage. On the other hand, too smooth seal countersurfaces result in poorer hydrodynamic lubrication of the sealing contact and, due to reduced conditioning of the sealing edge, impair the necessary active pumping effect of the sealing system. Consequently, this results in impaired sealing capability of the rotary shaft seal and increased thermal load on the system components of the rotary shaft seal system.

5.3 Lead – Fundamentals and Definitions

In sealing technology, lead refers to the entirety of structures on the seal countersurfaces of rotary shaft seals that pump the fluid to be sealed in an axial direction through the sealing gap during shaft rotation. The pumping direction depends on the rotation direction of the shaft and the lead orientation, and it can result in either leakage or insufficient lubrication of the sealing contact, see Figure 2. The designation of the lead orientation follows the definition of a screw thread as right-hand or left-hand lead. The associated parameters describe the lead orientation of a right-hand lead with a positive sign and a left-hand lead with a negative sign. For the definition of the shaft rotation direction Figure 2, the viewing direction is from the air side to the fluid side of the rotary shaft seal.

Legend	
1	Viewing direction
2	Air side of the rotary shaft seal
3	Fluid side of the rotary shaft seal
4	Counterclockwise (CCW) rotation direction
5	Clockwise (CW) rotation direction
6	Microlead
7	Macrolead
8	Pumping direction of the seal countersurface
9	Leakage
10	Insufficient lubrication

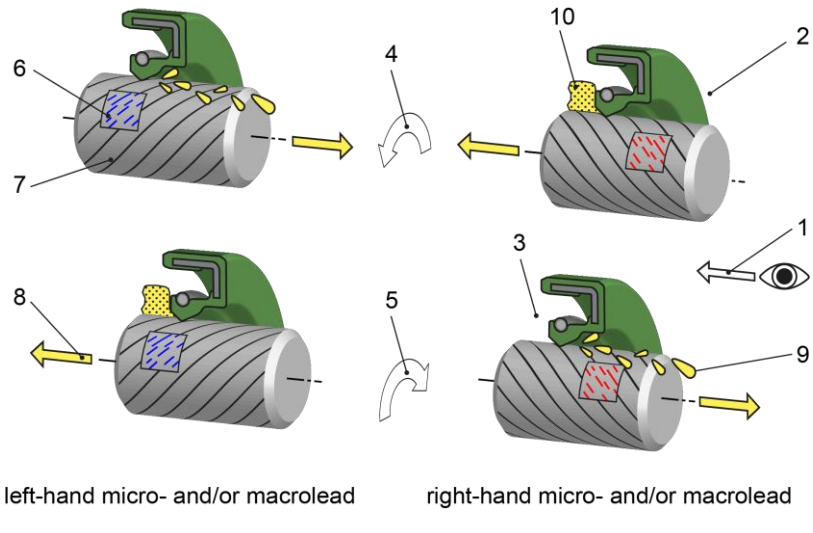

Figure 2: Illustration of the direction-dependent effects of lead on the seal countersurface: leakage and insufficient lubrication according to [17]

Different categories of lead can occur superimposed on ground seal countersurfaces. Table 1 provides an overview of these categories. Additionally, Figure 3 depicts an exemplary topography for each lead category.

Table 1: Overview of lead categories

Category	Characteristic
Microlead	Stochastically distributed grinding grooves, anisotropic, Figure 3 (a)
Periodic macrolead	Axially periodic grinding structures, anisotropic, thread-like in circumferential direction, Figure 3 (b)
Aperiodic macrolead	Aperiodic/stochastically distributed structures, anisotropic, circumferential/interrupted in circ. direction, Figure 3 (c)
Surface imperfections	According to DIN EN ISO 8785 [10], e.g. grooves and scratches, Figure 3 (d)

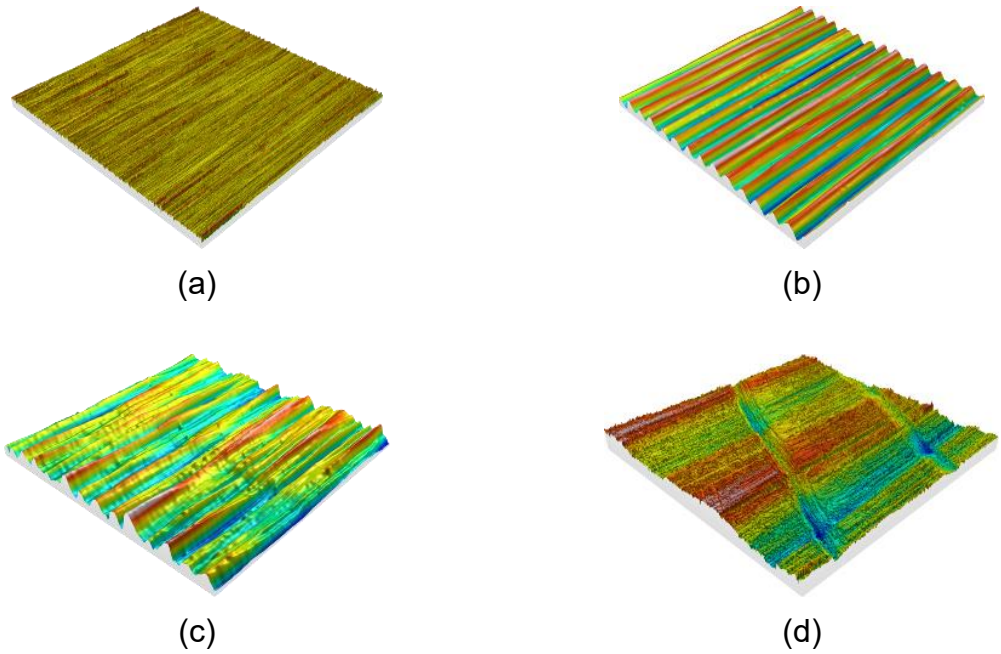

(a) (b) (c) (d)

Figure 3: Lead categories on seal countersurfaces

6 Measuring Methods for Surface Deviations

The surface deviations of seal countersurfaces are determined using geometry measurement data (form, roundness, etc.), axial 2D profiles (roughness and waviness) and areal topography measurement data (3D parameters). Relevant parameters and characteristics of the seal countersurface with regard to surface deviations are described in the following sections. For standardized determination, the procedure for the measurement, filtering and data processing must be defined. The roughness and form measurement are well-established in the industry and are not further elaborated here.

The following standards and guidelines are applied:

DIN EN ISO 3274 [11]	Profile Method
DIN EN ISO 16610-1 [12]	Filtration – Overview and basic concepts
DIN EN ISO 21920-1-3 [4–6]	Surface texture: Profile
DIN EN ISO 25178-1-3 [7–9]	Surface texture: Areal

Note 1: The default settings for determining the parameters of the roughness profile (R parameters, or roughness parameters) and the waviness profile (W parameters) are according to the setting classes in DIN EN ISO 21920-3. Default settings include the measurement and filter conditions of a profile. Ground seal countersurfaces for elastomer rotary shaft seals are within roughness in setting class Sc3, see DIN EN ISO 21920-3 Table 3. If no deviating specifications are indicated in the drawing specifications, these default settings are adopted.

Note 2: The DIN EN ISO 25178 standard does not define a fixed procedure for determining the 3D surface parameters. It is therefore essential that the filters and measurement conditions used are clearly specified and agreed.

6.1 R-Parameters for Describing the Seal Countersurface

6.1.1 Maximum Height of the Roughness Profile

Rz [µm]

To determine Rz, the roughness profile is divided into five equal sections in the axial direction, see DIN EN ISO 21920-3 Table 3. The Rz value represents the mean of the vertical differences from the deepest to the highest point within each section of the roughness profile.

6.1.2 Arithmetic Mean Roughness

Ra [µm]

The Ra value is calculated as the arithmetic mean of the absolute values of the profile values.

6.1.3 Maximum Height per Section of the Roughness Profile

Rzx [µm]

Rzx represents the maximum value of the vertical difference between the deepest and the highest point of a sliding section of length *l* through the roughness profile, see DIN EN ISO 21920-3, Table 7.

Note: Prior to the introduction of the maximum height per section of the roughness profile, Rzx, with the DIN EN ISO 21920-3 series, the maximum roughness height, Rmax, according to VDA 2006 was used.

6.2 W-Parameters for Describing the Seal Countersurface

6.2.1 Total Height of the Waviness Profile

Wt [µm]

Wt is the vertical difference from the deepest to the highest point of the waviness profile.

6.3 S-Parameters for Describing the Seal Countersurface

6.3.1 Maximum Height

Sz [µm]

Sz is the vertical difference from the deepest to the highest point of the scale-limited surface.

6.3.2 Arithmetic Mean Height

Sa [µm]

The Sa value is calculated as the arithmetic mean of the ordinate values of the scale-limited surface

6.4 Form Deviations of the Seal Countersurface

Geometric form deviations of the seal countersurface can be evaluated with a coordinate measuring machine or roundness measuring instrument. Relevant dimensions include diameter, roundness or circumferential waviness, and cylindricity of the shaft.

6.5 Damages to the Seal Countersurface

A visual inspection of the seal countersurface is recommended prior to the assembly of the sealing system. This ensures that the seal countersurface is free from any damage, including dents, scratches, cracks, rust and protrusions.

7 Measuring Methods for Lead

In regard to the measurement of lead, it is important to note that the individual measuring methods are only suitable for detecting specific lead categories. Additionally, a distinction is made between quantitative and qualitative methods. Table 2 provides an overview of the measurement and testing methods for lead, their detectable lead categories, and the type of result. For a comprehensive lead analysis, lead measuring methods must be combined. A comprehensive overview of the subject of “lead measurement” and the current state of knowledge regarding the functional description of the effects of lead is provided in reference [18].

Table 2: Overview of measurement and testing methods for lead with indication of suitability and type of result

	Suitability			Result	
Measuring Method	**Microlead**	**Macrolead**		**Qualitative**	**Quantitative**
		Periodic	**Aperiodic**		
7.1 Structure-based Microlead Analysis	X	--	--	--	X
7.2 Structure-based Macrolead Analysis	--	X	X	--	X
7.3 Macrolead Evaluation acc. to MBN 31007-7	--	X	--	--	X
7.4 Dominant Waviness according to VDA 2007	--	(X)[1]	--	--	X
7.5 Lead Testing with the Thread Method	X	X	X	X[2]	--
7.6 Lead Testing with the Scattered Light Method	--	X	--	X	--

[1] Only conditionally suitable, as the parameters are determined from individual profiles. Therefore, no macrolead angle can be determined, see Section 7.4

[2] Predominantly qualitative measuring method. A theoretical lead angle can be determined, but since the thread is influenced by all present superimposed lead categories, the differentiation of lead categories is not possible, see Section 7.5

Below, the measuring methods and their results are briefly described, and relevant parameters are listed. Detailed descriptions and further sources are explained in the annex.

7.1 Structure-based Microlead Analysis

The methodology of structure-based microlead analysis was developed within the FKM project series „Strukturanalyse“ [19–21]. In the process of structure-based microlead analysis, grinding grooves are separated, geometrically localized, and evaluated as geometric elements. Subsequently, a statistical evaluation is conducted to determine the structure-based microlead parameters and any associated diagram representations.

The measurement strategy for structure-based microlead analysis, as well as sample reports for documenting the measurement and evaluation results, are described in Annex A.1. Additionally, a strategy for combined measurement for structure-based evaluation of microlead and macrolead, as well as an overall "lead" report, are presented in Annex A.3.

The following sections provide an explanation of the structure-based microlead parameters.

7.1.1 Angular Distribution Curve and Angular Volume Distribution Curve

The angular distribution curve and the angular volume distribution curve represent the number or the volume of equally oriented grinding grooves accumulated over the angular orientation. In the diagrams, the zero-degree position indicates the circumferential direction of the shaft. Associated parameters for the angular distribution curve and angular volume distribution curve are the median angle of the angular distribution $Sd_{median,S}$, the median angle of the angular volume distribution $Sd_{median,V}$, and the standard deviation of the structure angle orientations Sd_{std}.

An optimal seal countersurface exhibits symmetrical and circumferentially oriented distribution curves with a defined minimum distribution width. Whether a left-hand or right-hand microlead is present can be identified by a shift or asymmetry in the distribution curves and thus an unequal distribution. A color-coding shows left-oriented grinding grooves as negative orientations (blue) and right-oriented grinding grooves as positive orientations (red).

Figure 4 shows three examples of different microlead-angular distribution curves. The parameters highlighted in red exceed the tolerance ranges outlined in Section 9. Complete report examples of the seal countersurfaces in Figure 4 are presented in Annex A.1.

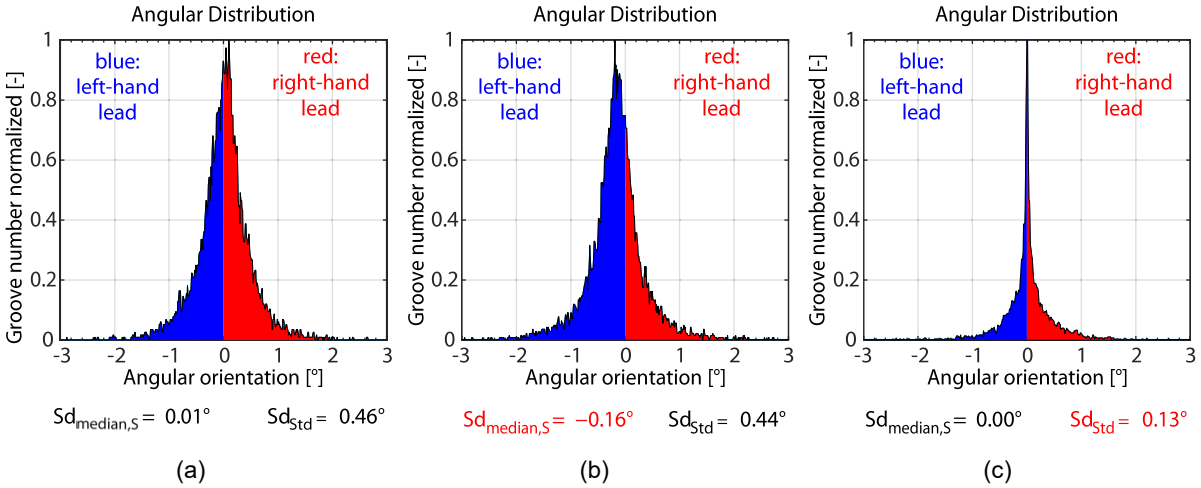

Figure 4: Examples of microlead-angular distribution curves:

(a) Symmetrical to the circumferential direction and with distribution width within the tolerance range – *microlead-free*;

(b) Shifted into the negative angle range – *left-hand microlead;*

(c) Symmetrical and circumferentially oriented with distribution width outside the tolerance range

7.1.2 Median Angle of the Microlead Angular Distribution

$Sd_{median,S}$ [°]

The median angle of the angular distribution $Sd_{median,S}$ indicates the angle value for which the number of larger and smaller structure angles is equal.

Note: Values in close proximity to 0.00° are optimal for $Sd_{median,S}$. This signifies a balanced state between left- and right-oriented structures, and the absence or minimal presence of a pumping effect.

7.1.3 Median Angle of the Microlead Angular Volume Distribution

$Sd_{median,V}$ [°]

The median angle of the angular volume distribution $Sd_{median,V}$ indicates the angle value for which the summed, oriented structure volume to the left and right of the angle value is equal.

Note: Values in close proximity to 0.00° are optimal for $Sd_{median,V}$. This signifies a balanced state between left- and right-oriented structures, and the absence or minimal presence of a pumping effect.

7.1.4 Standard Deviation of the Microlead Angular Distribution

Sd_{std} [°]

The standard deviation Sd_{std} is used as a statistical measure for the scatter of the structure angle orientations. It quantifies the width of the angular distribution curve and is derived from a Gaussian curve fitted to the normalized angular distribution.

Note: Larger values of the standard deviation Sd_{std}, and, consequently, wider angular distributions, are advantageous. The fluid exchange in the sealing gap is facilitated, and potential shifts of the distribution in one direction have a less significant impact on the absolute percentage of structures oriented left or right. This indicates that wider distributions have more robust properties for sealing.

7.1.5 Arithmetic Mean of the Microlead Depth

Sd_t [µm]

Sd_t is the arithmetic mean depth of all detected microlead structures.

Note: Deeper structures result in higher pumping rate, as they can hold and pump a larger amount of fluid.

7.1.6 Percentage of Left- and Right-Oriented Microlead Structures

$Sd_{Sum,li}$ / $Sd_{Sum,re}$ [%]

$Sd_{Sum,li}$ and $Sd_{Sum,re}$ represent the percentages of the sums of left- and right-oriented microlead structures of the angular distribution curve.

7.1.7 Percentage of Left- and Right-Oriented Structural Volume

$Sd_{Vol,li}$ and $Sd_{Vol,re}$ represent the percentages of the left- and right-oriented cumulative structural volume of the angular volume distribution.

7.1.8 Number of Microlead Structures per Square Millimetres

$Sd_{Sum,tot}$ [1/ mm^2]

$Sd_{Sum,tot}$ represents the total number of microlead structures identified within an area of 1 mm².

7.2 Structure-based Macrolead Analysis

The measurement and evaluation methodology of the structure-based macrolead analysis was developed in the FVA 876 project „3D-Makrodrall“ [22]. In the analysis process, macrolead structures are localized in 3D topographies and evaluated as geometric elements. These structures can exhibit both periodic and aperiodic characteristics. Subsequent statistical evaluation yields the structure-based macrolead parameters and associated representations.

The measurement strategy for structure-based microlead analysis, as well as sample reports for documenting the measurement and evaluation results, are described in Annex A.2. Additionally, a strategy for combined measurement for structure-based evaluation of microlead and macrolead, as well as an overall "lead" report, are presented in Annex A.3.

The following sections provide an explanation of the structure-based macrolead parameters

7.2.1 Median of Structure Angles

$SD\gamma_{median}$ [°]

$SD\gamma_{median}$ is the median value of the structure angles of all detected structures.

Note: $SD\gamma_{median}$ should show values close to 0.00° in order to achieve a balance state between left and right oriented structures. This ensures that an axial pumping effect of the structures is avoided or at least minimized.

7.2.2 Standard Deviation of Structure Angles

$SD\gamma_{std}$ [°]

$SD\gamma_{std}$ is the standard deviation of the structure angles of all detected structures and a measure of the scatter of the structure angles.

Note 1: The presence of highly oriented structures is indicated by low values of $SD\gamma_{std}$. As the standard deviation increases, the scatter of the individual structure angles and the degree of the isotropy of the surface also increase.

Note 2: In general, larger standard deviations of structure angles $SD\gamma_{std}$ result in more stable sealing conditions and facilitate fluid exchange in the sealing gap.

7.2.3 Mean of Structure Widths

SDB_{mean} [µm]

SDB_{mean} corresponds to the mean width of the structures of all detected structures.

Note 1: Smaller structure widths SDB_{mean} result in a higher number of structures being active in the sealing contact, thereby enabling higher pumping rates of the seal countersurface to be achieved.

Note 2: In order to assess the seal countersurface, it is necessary to consider the mean structure width SDB_{mean} in conjunction with the standard deviation of the structure widths $SDB_{std.}$

7.2.4 Standard Deviation of Structure Widths

SDB_{std} [µm]

SDB_{std} is the standard deviation of the structure widths of all detected structures and a measure of the scatter of the structure widths.

Note 1: Lower values of SDB_{std} indicate that all structures have similar structure widths, which allows for the conclusion to be drawn about axial periodicity. Conversely, larger values of SDB_{std} indicate a decrease in the degree of periodicity, leading to a classification of the surface structures as aperiodic.

Note 2: In order to assess the seal countersurface, it is necessary to consider the mean structure width SDB_{mean} in conjunction with the standard deviation of the structure widths SDB_{std}.

7.2.5 Coefficient of Variation of Structure Widths

$VarK_{SDB}$ [-]

The coefficient of variation of structure widths, denoted as $VarK_{SDB}$, is calculated as the ratio of the standard deviation of structure widths SDB_{std} to the arithmetic mean structure width SDB_{mean}.

$$\mathrm{VarK_{SDB}} = \frac{\mathrm{SDB_{std}}}{\mathrm{SDB_{mean}}}$$

$VarK_{SDB}$ is a relative measure of the scatter of structure widths and serves as an indicator for the presence of an axial periodic structure on the surface. The strength of the axial periodic expression decreases from 0 upwards.

7.2.6 Mean of Structure Depths

SDT_{mean} [µm]

SDT_{mean} corresponds to the mean depth of all detected structures.

Note: Deeper structures result in higher pumping rate, as they can hold and pump a larger amount of fluid.

7.2.7 Ratio of the Mean Structure Length to the Measuring Field Length

$SDL_{mean,n}$ [-]

$SDL_{mean,n}$ is the ratio of the determined average structure length SDL_{mean} to the length of the measuring field in the circumferential direction l_y.

$$\mathrm{SDL_{mean,n}} = \frac{\mathrm{SDL_{mean}}}{l_y}$$

This parameter qualitatively indicates whether there are circumferential continuous or circumferentially interrupted structures, which corresponds to a distinction between periodic and aperiodic macrolead.

7.2.8 Structure Angular Distribution

The structure angular distribution is a histogram that represents the number of structures with the identical structure angle accumulated over the angular orientation. In the diagrams, the zero-degree position indicates the circumferential direction of the measured shaft. The median of the structure angles $SD\gamma_{med}$ and the standard deviation of the structure angles $SD\gamma_{std}$ are associated parameters for the structure angular distribution.

An optimal seal countersurface is characterized by a symmetrical structure angular distribution around the zero-degree position, with a broad scatter. A left-hand or right-hand macrolead can be identified by an unequal distribution of the structure angles around the zero-degree position. A color-coding shows left-oriented structures as negative orientations (blue) and right-oriented structures as positive orientations (red).

Figure 5 shows two examples of different structure angular distributions. The parameters highlighted in red exceed the tolerance ranges outlined in Section 9. Complete report examples of the seal countersurfaces in in Figure 5 are presented in Annex A.2.

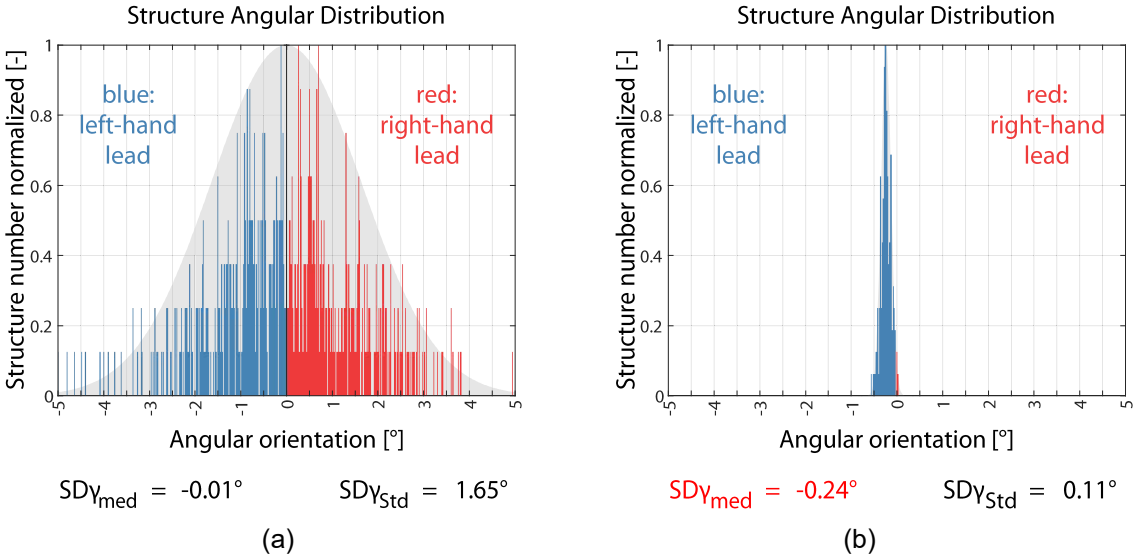

Figure 5: Examples of structure angular distributions:

(a) Symmetrical to the circumferential direction and with a broad scatter of individual orientations – *macrolead-free;*

(b) Almost entirely shifted into the negative angle range and with a narrow distribution width, predicted pumping effect – *periodic or aperiodic macrolead*

7.2.9 Structure Width Distribution

The distribution of structure widths is represented by a histogram, which illustrates the number of structures with identical structure widths. This representation can illustrate various distribution characteristics of the structures on the seal countersurface.
Two different examples are shown in Figure 6. Complete report examples of the seal countersurfaces in Figure 6 are presented in Annex A.2.

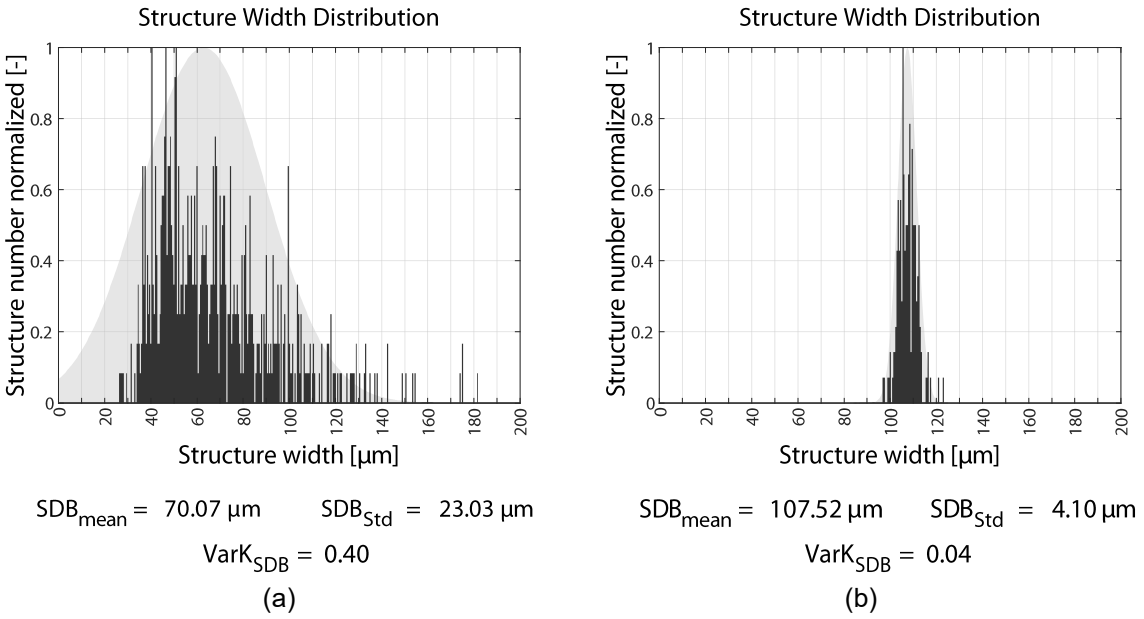

Figure 6: Examples of structure width distributions:

(a) Wide range of occurring structure widths without recognizable regularity in the distribution – *macrolead-free or aperiodic macrolead;*

(b) Normally distributed structure widths with a narrow distribution width – *periodic macrolead.*

7.3 Macrolead Evaluation according to MBN 31007-7

The Mercedes-Benz factory standard MBN 31007-7 [13] describes a measurement and evaluation method for the quantitative detection of axially periodic, circumferential macrolead. The seal countersurface is measured using a defined measurement grid of axial surface profiles around the circumference of the shaft. The FFT (Fast Fourier Transform) analysis is employed to determine dominant frequencies of the surface measurement data. These frequencies are subsequently summarized in a mathematical initial function, which is then approximated to the surface. The macrolead parameters according to MBN 31007-7 are then determined based on the resulting mathematical approximated lead surface.

The measurement strategy for the macrolead evaluation according to MBN 31007-7, as well as sample reports for documenting the measurement and evaluation results, are described in Annex A.4.

The following sections provide an explanation of the relevant macrolead parameters according to MBN 31007-7.

7.3.1 Lead Angle

Dγ [°]

Dγ is the angle between the circumferential direction of the shaft and the lead structure.

Note: A positive angle indicates a right-hand lead, while a negative angle indicates a left-hand lead.

7.3.2 Period Length

DP [mm]

DP is the distance between two successive wave peaks or wave troughs in the axial direction.

Note: Smaller period lengths DP result in a larger number of structures being active in the sealing contact, thereby creating a higher pumping effect.

7.3.3 Lead Depth

Dt [µm]

Dt is the maximum vertical distance between the wave peak and wave trough.

Note: Deeper structures result in higher pumping rate, as they can hold and pump a larger amount of fluid.

7.3.4 Number of Threads

DG [-]

DG is the number of periods in the circumferential direction, based on 360°.

Notes: The number of threads DG considers the lead angle Dγ, the period length DP, and the shaft diameter in a single value.

7.3.5 Theoretical Supply Cross Section

DF [µm^2]

DF is the cross-sectional area of a period length in an axial section of the lead surface.

7.4 Dominant Waviness according to VDA 2007

The VDA 2007 Guideline [15] from the German Association of the Automotive Industry (VDA) defines an algorithmic evaluation method for periodic surface structures. The method employs band-pass filtering to analyze existing periodic components in a surface profile. The surface profiles are measured according to the profile method outlined in DIN EN ISO 3274 [11] or via optical measurement. The parameters can be used to detect periodic macrolead. A comprehensive description of periodic macrolead is not provided, as the determination of a lead angle is not possible.

Note 1: The evaluation method identifies the dominant characteristics of the period lengths of the axial measurement length ln in the range of 0.02 mm ≤ WDSm ≤ ln/5.

Note 2: If a dominance with an average height of the profile elements of WDc ≥ 0.3 µm is detected, the seal countersurface should be examined for macrolead using the macrolead analysis according to MBN or the 3D macrolead analysis.

7.4.1 Horizontal Waviness

WDSm [µm]

WDSm is the average period length of the dominant waviness determined from the amplitude spectrum.

7.4.2 Total Height of the Waviness Profile

WDt [µm]

WDt is the vertical difference between the highest and lowest points of the WD profile.

7.4.3 Average Height of Profile Elements

WDc [µm]

WDc is the average of the vertical differences between the highest and lowest points of the profile elements (average height of the waviness peaks).

7.5 Lead Testing with the Thread Method

The thread method is a primarily qualitative testing procedure for detecting both macrolead and microlead on seal countersurfaces. The presence of lead is evaluated based on the movement of a thread wrapped around the horizontally clamped, rotating seal countersurface. If the thread moves in the axial direction, this indicates lead on the seal countersurface. The test setup and test specifications are detailed in Annex A.5

It is not possible to distinguish between macrolead and microlead on the seal countersurface using the thread method, as the thread is influenced integrally by the surface. In the worst case, a superposition of, for example, right-hand macrolead and left-hand microlead may result in the thread not moving axially, which would yield a false-negative result.

7.5.1 Procedure for the Thread Method

1) The shaft to be measured is clamped horizontally in a chuck and aligned, if necessary, with the aid of a tailstock.

2) A thread is then wrapped around the seal countersurface and weighted with a defined weight.

3) Over a specified time interval, the seal countersurface is rotated in direction 1 at a defined rotational speed, and the thread is observed. If the thread moves, the direction and distance passed over are documented.

4) Over the same time interval and with the same rotational speed, the seal countersurface is rotated in the opposite direction 2, and the thread is observed. If the thread moves, the direction and distance passed over are documented.

Note: It is recommended that a digital camera with a magnifying lens is used for the observation and documentation of the thread movement and the determination of the distance passed over by the thread.

7.5.2 Evaluation of the Thread Method

A left-hand or right-hand lead on the seal countersurface is determined according to Table 3. In order to achieve a distinct result, it is essential that the directions of thread movement in rotation direction 1 and rotation direction 2 are opposite.

Table 3: Result of the thread method according to the directional conventions in Figure 2

	Rotation direction counter clockwise (CCW)	**Rotation direction clockwise (CW)**	**Integral Lead Orientation**
Axial direction of the thread movement	right	left	left-hand lead
	left	right	right-hand lead

Note 1: If the measured axial distances in rotation direction 1 and rotation direction 2 are not comparable, or the thread moves in the same direction in both cases, this may indicate incorrect clamping of the shaft or waviness or form deviation of the seal countersurface.

Note 2: If thread movement is identified through the thread method, it is recommended to further quantitatively examine the seal countersurface for microlead and macrolead. This is the only way to accurately specify and describe the lead category on the seal face.

7.5.3 Parameters of the Thread Method

A procedure for determining a lead angle Φ based on the thread method is documented in the OS 1-1 Guideline of the RMA [16]. The following measurement parameters are required:

D	[mm]	Diameter of the shaft
X	[mm]	Axial distance of the thread movement
N	[U/min]	Rotation speed
t	[s]	Test duration

Equation for calculating the lead angle Φ:

$$\Phi = \tan^{-1}\left(\frac{X \cdot 60s}{\pi \cdot D \cdot N \cdot t}\right)$$

Note: The result of the thread method depends on the equipment and user. In addition, the lead angle Φ is not directly comparable to the angle parameters of quantitative methods. Operator influence, superimposed lead categories, and nonvisible influencing factors affect the result.

7.6 Lead Testing with the Scattered Light Method

The scattered light method uses the principle of scattered light measurement technology to detect periodic macrolead. By analyzing the diffraction pattern of a laser beam reflected from the seal countersurface, conclusions can be drawn about axially periodic structures on the surface. The functionality of a handheld device allows for its application under manufacturing conditions.

If a periodic structure is detected using the scattered light method, it is recommended to further quantitatively examine the seal countersurface for macrolead.

7.6.1 Parameters of the Scattered Light Method

The diffraction pattern can be used to indirectly determine the period length DP, and lead depth Dt according to [23]. However, it is not possible to determine a lead angle due to the functional principle.

8 Procedure for Analyzing a Seal Countersurface

The analysis of seal countersurfaces can be conducted in accordance with the sequence illustrated in Figure 7. For a comprehensive analysis result, it is essential to examine the seal countersurface for surface imperfections, surface deviations, macrolead, and microlead.

Qualitative methods can only indicate the presence of lead or other harmful surface features. If methods with quantitative results are available, they provide distinct measurement results, thus offering a more detailed description of the seal countersurface.

It is recommended to carry out a comprehensive lead and surface analysis after, for example, modifications to the grinding process (process approval), when using new grinding tools or other machine adaptions, as well as in case of failure after leakage in rotary shaft sealing systems.

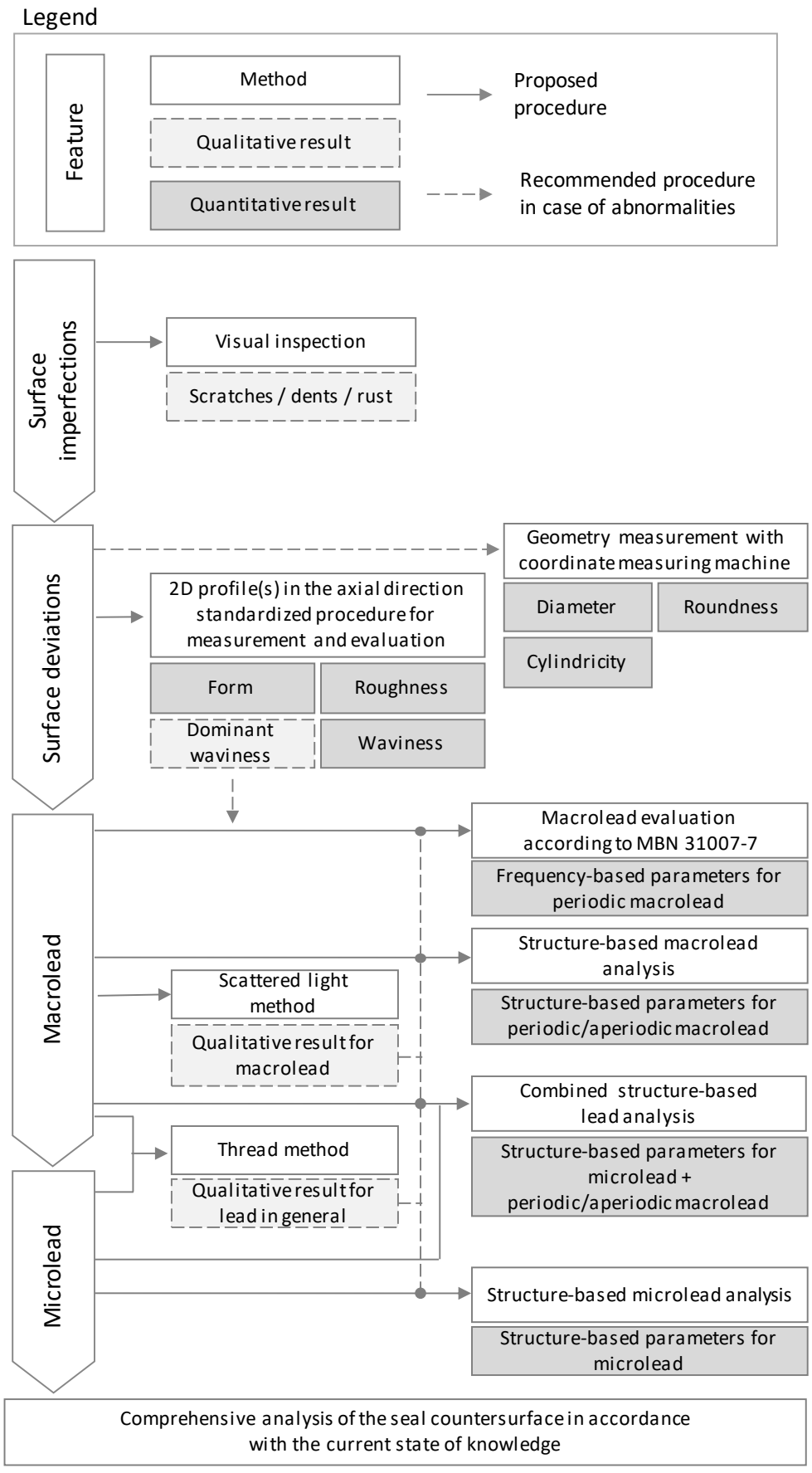

Figure 7: Procedure for analyzing the surface of a seal countersurface

9 Example Drawing Specifications

The drawing specification is made using the basic surface tolerance symbol with a cross line for material-removing machining. The symbol for profile (line) or areal (parallelogram) surface texture is shown above it. The measurement conditions and limits depend on the component part, the application conditions, and the type and design of the rotary shaft seal.

9.1 Example Drawing Specifications for Roughness and Waviness according to DIN EN ISO 21920

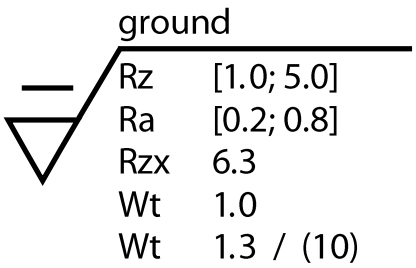

General information: Unless otherwise specified, the measurement conditions and filter parameters are based on the default settings of the setting class *Sc3* in DIN EN ISO 21920-3. Line 5 is an example of an alternative measurement condition.	
1. Line	The lower tolerance limit for the maximum height of the roughness profile is Rz = 1.0 µm, upper tolerance limit is Rz = 5.0 µm.
2. Line	The lower tolerance limit for the arithmetic mean height of the roughness profile is Ra = 0.2 µm, the upper tolerance limit is Ra = 5.0 µm.
3. Line	The upper tolerance limit for the maximum height per section of the roughness profile is Rzx = 6.3 µm.
4. Line	The upper tolerance limit for the total height of the waviness profile is Wt = 1.0 µm.
5. Line	The upper tolerance limit for the total height of the waviness profile over a measurement length of 10 mm is Wt =1.3 µm.

9.2 Example Drawing Specifications for Structure-based Microlead Analysis

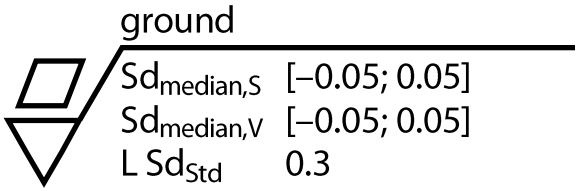

1. Line	The lower tolerance limit of the median angle of the angular distribution is $Sd_{median,S}$ = –0.05°, the upper tolerance limit is $Sd_{median,S}$ = 0.05.
2. Line	The lower tolerance limit of the median angle of the angular volume distribution is $Sd_{median,V}$ = –0.05°, the upper tolerance limit is $Sd_{median,V}$ = 0.05.
3. Line	The lower tolerance limit of the standard deviation of the angular distribution is Sd_{std} = 0.3°.

9.3 Example Drawing Specifications for Structure-Based Macrolead Analysis

1. Line	The lower tolerance limit of the median of the structure angles is $SD\gamma_{median}$ = –0.1°, the upper tolerance limit is $SD\gamma_{median}$ = 0.1°.
2. Line	The upper tolerance limit of the mean of structure depths is SDT_{mean} = 1.0 µm.
3. Line	The lower tolerance limit of the coefficient of variation of structure widths is $VarK_{SDB}$ = 0.2 µm.

9.4 Example Drawing Specifications for Macrolead Evaluation according to MBN 31007-7

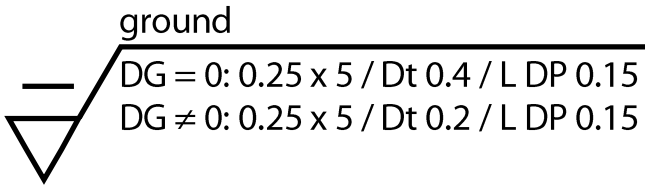

1. Line	If the number of threads DG = 0, a lead depth Dt = 0.4 µm must not be exceeded. The lower tolerance limit of the period length is DP = 0.15 mm. The period length is valid within a range of 0.02 mm to 0.25 mm.
2. Line	If the number of threads DG ≠ 0, a lead depth Dt = 0.2 µm must not be exceeded. The lower tolerance limit of the period length is DP = 0.15 mm. The period length is valid within a range of 0.02 mm to 0.25 mm.

Note 1: The validity range defines the period length range indicated by the drawing specification within which the lead parameters are evaluated. Lead characteristics with period lengths outside the specified validity range are not evaluated.

Note 2: The drawing specification in front of the lead parameter(s) specifies the validity range. The smallest evaluable period length is 0.02 mm. If the validity range is defined with this default lower limit, this value does not have to be specified in the drawing specification, only the upper limit.

Note 3: If no validity range is specified in the drawing specification, the default validity range is 0.02 to 0.4 mm.

Literature reference

[1] **Deutsches Institut für Normung e.V.:** DIN 3760: *Radial-Wellendichtringe*, Berlin. September 1996.

[2] **Deutsches Institut für Normung e.V.:** DIN 3761-2: *Radial-Wellendichtringe für Kraftfahrzeuge - Anwendungshinweise*, Berlin: Beuth. November 1983.

[3] **Deutsches Institut für Normung e.V.:** DIN 4760: *Gestaltabweichungen - Begriffe; Ordnungssystem*: Beuth. Juni 1982.

[4] **Deutsches Institut für Normung e.V.:** DIN EN ISO 21920-2: *Geometrische Produktspezifikation (GPS) - Oberflächenbeschaffenheit: Profile - Teil 2: Begriffe und Kenngrößen für die Oberflächenbeschaffenheit*, Berlin: Beuth. Dezember 2022.

[5] **Deutsches Institut für Normung e.V.:** DIN EN ISO 21920-1: *Geometrische Produktspezifikation (GPS) - Oberflächenbeschaffenheit: Profile - Teil 1: Angabe der Oberflächenbeschaffenheit*, Berlin: Beuth. Dezember 2022.

[6] **Deutsches Institut für Normung e.V.:** DIN EN ISO 21920-3: *Geometrische Produktspezifikation (GPS) - Oberflächenbeschaffenheit: Profile - Teil 3: Spezifikationsoperatoren*, Berlin: Beuth. Dezember 2022.

[7] **Deutsches Institut für Normung e.V.:** DIN EN ISO 25178-3: *Geometrische Produktspezifikation (GPS) - Oberflächenbeschaffenheit: Flächenhaft - Teil 3: Spezifikationsoperatoren*: Beuth, 17.040.30. November 2012.

[8] **Deutsches Institut für Normung e.V.:** DIN EN ISO 25178-2: *Geometrische Produktspezifikation (GPS) - Oberflächenbeschaffenheit: Flächenhaft - Teil 2: Begriffe und Kenngrößen für die Oberflächenbeschaffenheit*: Beuth, 17.040.30. September 2023.

[9] **Deutsches Institut für Normung e.V.:** DIN EN ISO 25178-1: *Geometrische Produktspezifikation (GPS) - Oberflächenbeschaffenheit: Flächenhaft - Teil 1: Angabe von Oberflächenbeschaffenheit*: Beuth, 17.040.30. Dezember 2016.

[10] **Deutsches Institut für Normung e.V.:** DIN EN ISO 8785: *Geometrische Produktspezifikation (GPS) - Oberflächenunvollkommenheiten; Begriffe, Definition und Kenngrößen*: Beuth. Oktober 1999.

[11] **Deutsches Institut für Normung e.V.:** DIN EN ISO 3274: *Geometrische Produktspezifikation (GPS) - Oberflächbeschaffenheit: Tastschnittverfahren - Nenneigenschaften von Tastschnittgeräten*: Beuth. April 1998.

[12] **Deutsches Institut für Normung e.V.:** DIN EN ISO 16610-1: *Geometrische Produnktspezifikation (GPS) - Filterung; Teil 1: Überblick und grundlegende Konzepte*: Beuth. November 2015.

[13] **Mercedes-Benz:** Norm MBN 31007-7: *Geometrische Produktspezifikationen (GPS) - Oberflächenbeschaffenheit Mess- und Auswerteverfahren zur Bewertung von drallreduzierten dynamischen Dichtflächen.* September 2008.

[14] **Verband der Automobilindustrie e.V. (VDA):** VDA 2006: *Geometrische Produktspezifikation - Oberflächenbeschaffenheit; Regeln und Verfahren zur Beurteilung der Oberflächenbeschaffenheit.* Juli 2003.

[15] **Verband der Automobilindustrie e.V. (VDA):** VDA 2007: *Geometrische Produktspezifikation - Oberflächenbeschaffenheit; Definitionen und Kenngrößen der dominanten Welligkeit.* Februar 2007.

[16] **Rubber Manufacturers Association:** Technical Bulletin RMA OS-1-1: *Shaft Finish Requirements for Radial Lip Seals.* 2004.

[17] **Bauer, F.:** *Federvorgespannte-Elastomer-Radial-Wellendichtungen. Grundlagen der Tribologie & Dichtungstechnik, Funktion und Schadensanalyse*, Wiesbaden, Heidelberg: Springer Vieweg, 2021, Springer Fachmedien Wiesbaden, - ISBN 978-3-658-32922-8.

[18] **Baumann, M.:** *Abdichtung drallbehafteter Dichtungsgegenlaufflächen - Messung, Analyse, Bewertung und Grenzen*. Dissertation, 2017, Universität Stuttgart, Institut für Maschinenelemente, - ISBN 978-3-936100-69-3.

[19] **Baitinger, G.; Haas, W.:** *Strukturanalyse. Drall- und Mikrostrukturanalyse zur funktionalen Bewertung von Dichtringgegenlaufflächen*. Abschlussbericht FKM Vorhaben Nr. 285, AiF-Nr. 15628 N/1, Frankfurt am Main: FKM, 2011, Forschungskuratorium Maschinenbau e.V. (FKM).

[20] **Baumann, M.; Bauer, F.:** *Strukturanalyse III. Anwendung von Strukturanalyse und Festlegung von Qualitätskriterien für die gezielte Bewertung von Dichtungsgegenlaufflächen*. Abschlussbericht FKM Vorhaben Nr. 308, IGF-Nr. 18186 N, Frankfurt am Main: FKM, 2017, Forschungskuratorium Maschinenbau e.V. (FKM).

[21] **Baumann, M.; Bauer, F.; Haas, W.:** *Strukturanalyse II. Ganzheitliche, funktionale Bewertung von Dichtungsgegenlaufflächen mittels Strukturanalyse unter Einbeziehung der Wirkung von Strukturen auf die Förderwirkung der Welle*. Abschlussbericht FKM Vorhaben Nr. 298, IGF-Nr. 17138 N/1, Frankfurt am Main: FKM, 2015, Forschungskuratorium Maschinenbau e.V. (FKM).

[22] **Engelfried, M.; Baumann, M.; Bauer, F.:** *3D-Makrodrall - Strukturbasierte 3D-Analyse von Makrodrall*. Forschungsheft 1471, Forschungsvereinigung Antriebstechnik e.V., Abschlussbericht FVA Vorhaben Nr. 876 I, Frankfurt am Main, 2022.

[23] **Hertzsch, A.; Kröger, K.; Großmann, M.:** *Schnelle optische Drallmessung*. tm – Technisches Messen. 2013, 80 (12).

Annex

A.1. Annex for Structure-based Microlead Analysis

A.1.1. Measurement Strategy for Structure-based Microlead Analysis

High-resolution, area-based optical measuring methods are required for measuring microlead. Suitable measuring methods include white light interferometry or confocal microscopy.

The measurement grid for analyzing microlead consists of measuring fields distributed along the shaft axis and around the shaft circumference. To accomplish this, a motorized axis of the measuring device in the axial direction of the shaft as well as a motorized rotation axis are required.

A measurement grid for the detection of microlead on the seal countersurface must meet the following criteria:

1) For a statistically reliable statement, the measuring fields must contain a sufficient number of microscopic grinding grooves. The number depends on the measuring field size and the number of measuring fields.

2) To detect and compensate for angular errors due to a misalignment of the shaft multiple measurements in the axial and circumferential directions are necessary (wobble compensation).

To meet these criteria, it has been proven to measure the seal countersurface with an 18x3 measurement grid consisting of 18 measuring fields in the circumferential direction at intervals of ΔΦ = 20° at three axial positions at intervals of ΔX = 2 mm.

Note: The latest findings in the course of developing the combined measurement grid for lead show that measurement grids with a reduced number of measuring fields also achieve sufficient accuracy.

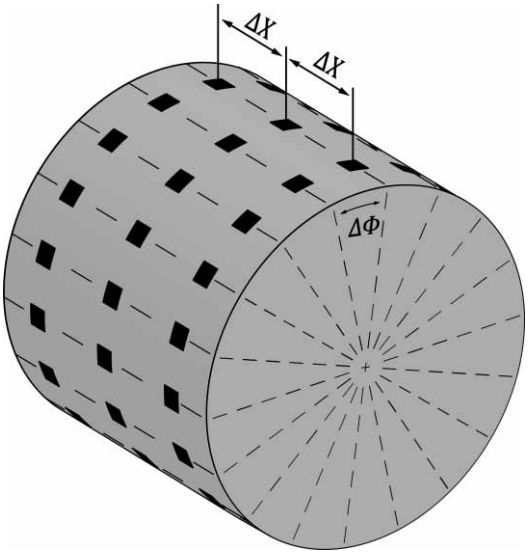

Figure 8: Proven measurement grid for structure-based microlead analysis

Table 4: Measurement conditions for structure-based microlead analysis

Measurement method	optical
Field size	min. 500 x 500 µm
Lateral resolution	< 1.5 µm
Vertical resolution	< 10 nm

Table 5: Measurement grid for structure-based microlead analysis

Number of circ. positions	18
Distance btw. circ. pos.	ΔΦ = 20°
Number of axis positions	3
Distance btw. axis pos.	ΔX = 2 mm

A.1.2. Report Examples for Structure-Based Microlead Analysis

Measurement Report IMA-Microlead®Analysis

Part:	Pass Example	Date:	DD-MM-YYYY HH:mm:ss		Spacer Logo
Editor:	Name	Device:	Confovis Lead Inspect		
Customer:	Name	Version:	V3.2	Mount:	

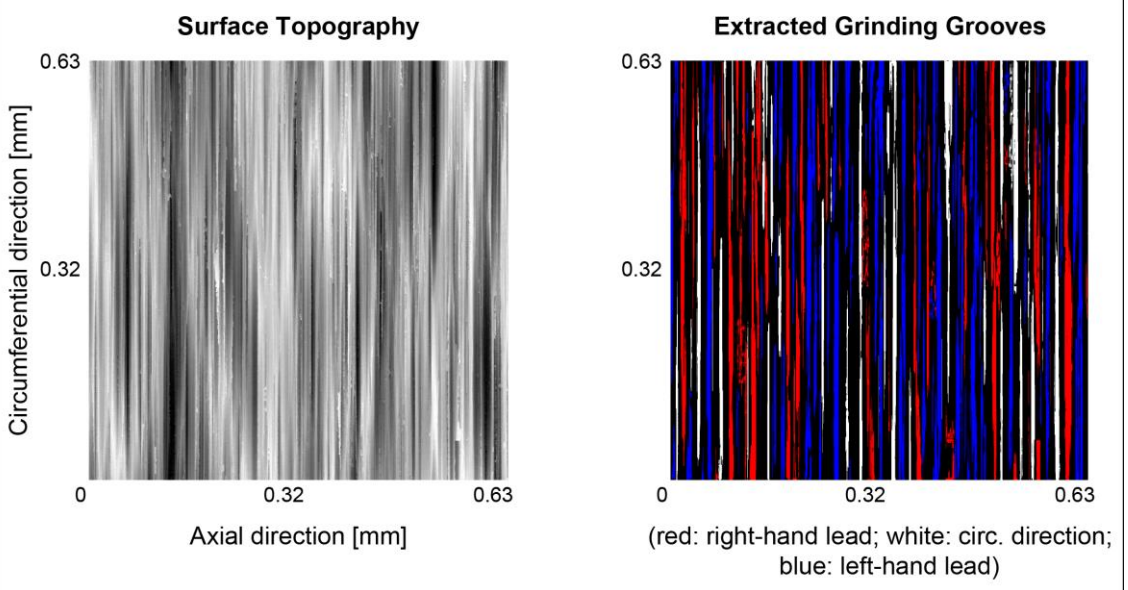

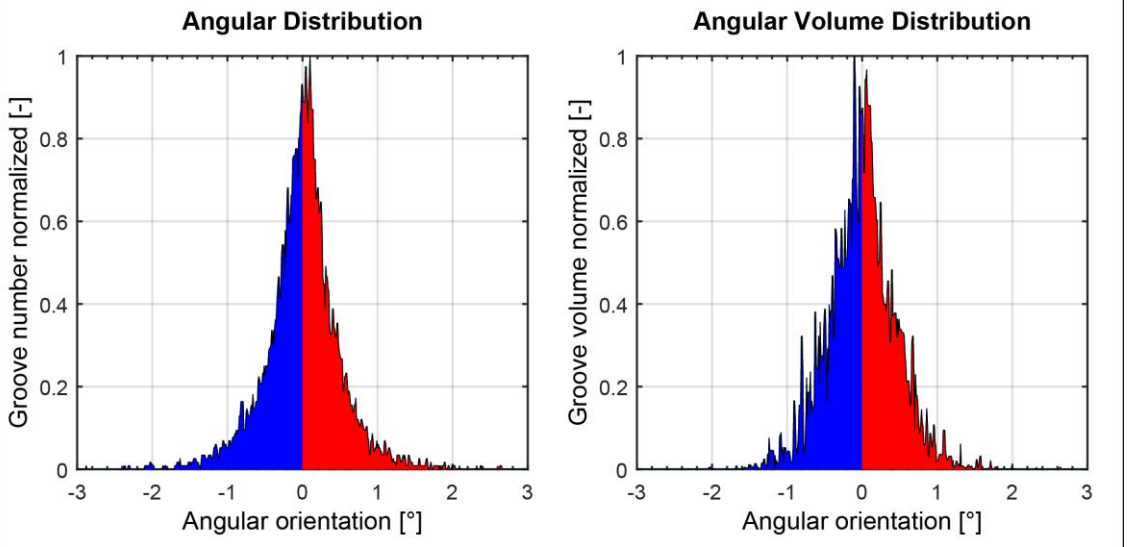

$Sd_{Sum,li}$ [%]	$Sd_{Sum,re}$ [%]	$Sd_{median,S}$ [°]	$Sd_{Vol,li}$ [%]	$Sd_{Vol,re}$ [%]	$Sd_{median,V}$ [°]
48	52	0.01	50	50	-0.01

Sd_t [µm]	Sd_{Std} [°]	$Sd_{Sum,tot}$ [$1/mm^2$]
0.48	0.46	402

Figure 9: Report of the structure-based microlead analysis of a pass example

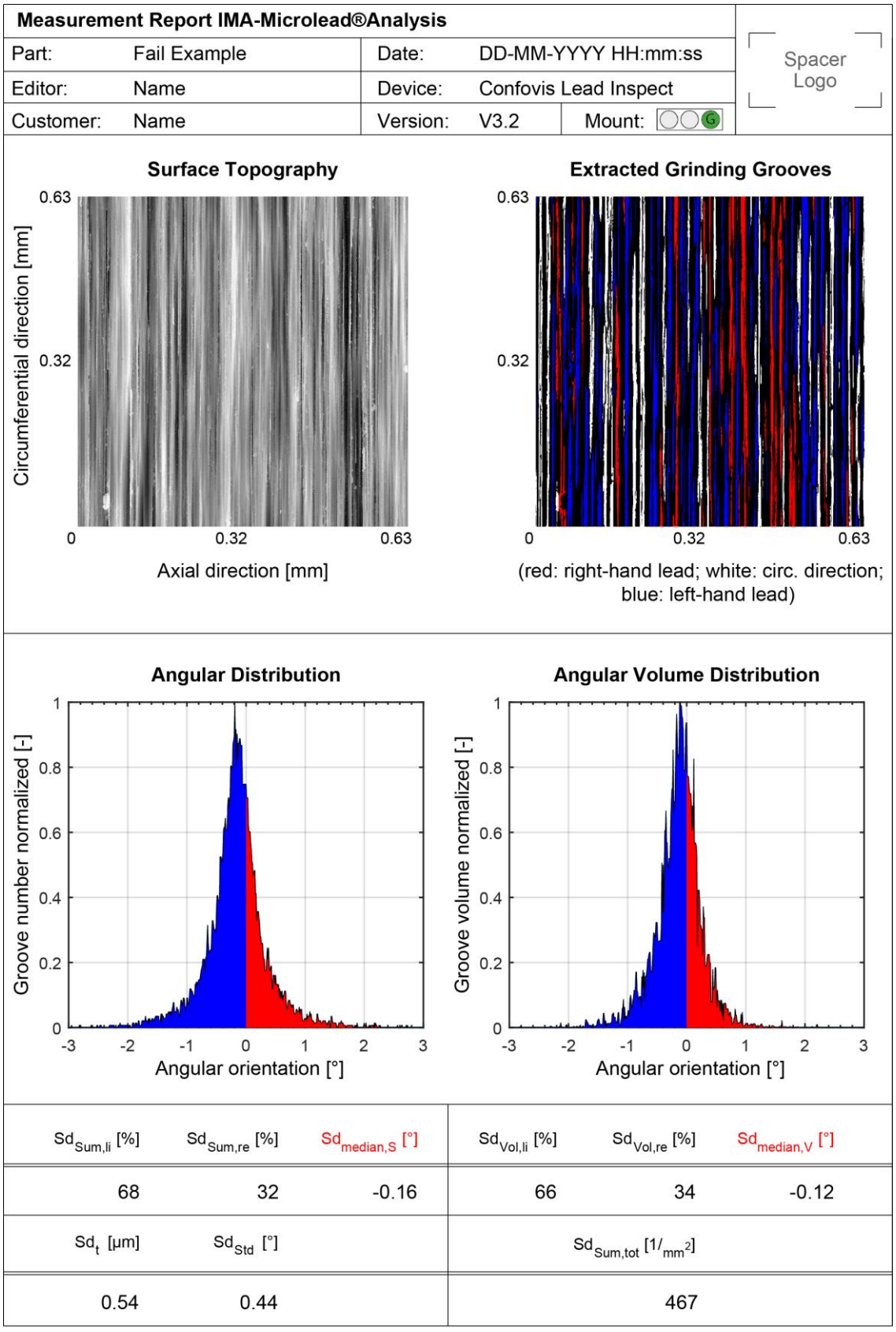

Figure 10: Report of the structure-based microlead analysis of a fail example

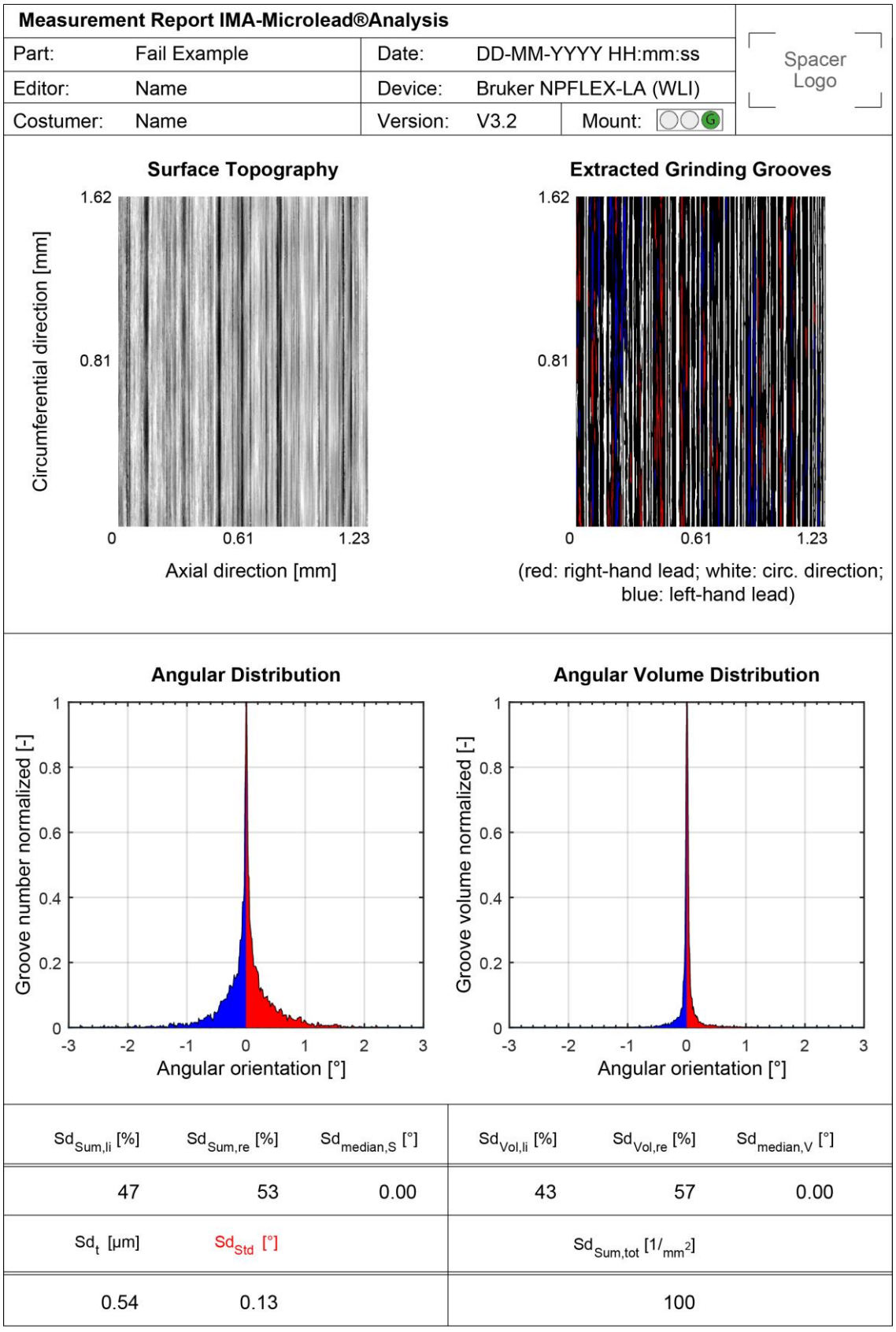

Figure 11: Report of the structure-based microlead analysis of a fail example

A.2. Annex for Structure-based Macrolead Analysis

A.2.1. Measurement Strategy for Structure-based Macrolead Analysis

High-resolution, area-based optical measuring methods are required for measuring macrolead. Suitable measuring methods include white light interferometry or confocal microscopy.

The measurement grid for analyzing macrolead consists of measuring fields distributed along the shaft axis and around the shaft circumference. To accomplish this, a motorized axis of the measuring device in the axial direction of the shaft as well as a motorized rotation axis are required.

A measurement grid for the detection of periodic and aperiodic macrolead on the seal countersurface must meet the following criteria:

1) For a statistically reliable statement, the measuring fields must contain a sufficient number of microscopic grinding grooves. The number depends on the measuring field size and the number of measuring fields.

2) The surface topographies must be of sufficient length in the circumferential direction in order to enable an accurate assessment of the course of the structures and their orientation.

3) In order to detect and compensate for angular errors due to a misalignment of the shaft, multiple measurements in the axial and circumferential directions are necessary (wobble compensation).

Note: The minimum field sizes required for structure-based macrolead analysis are larger than those required for structure-based macrolead analysis. This is due to the fact that macrolead covers a wide range of larger structure sizes and can exhibit variety of structure courses and distributions on the surface.

To meet these criteria, it is recommended to measure the seal countersurface with a 9x2x3 measurement grid consisting of nine measurement positions in the circumferential direction at intervals of $\Delta\Phi = 40°$ at two axial positions at intervals of $\Delta X = 4$ mm. At each measurement position, three circumferentially overlapping measuring fields are recorded. The stitching of individual measuring fields with the instrument's own stitching function can be employed to achieve the required measuring field size.

These overlapping measurements are combined into a stitched topography for each measurement position within the structure-based macrolead analysis and evaluated as such. The angular misalignments of the shaft due to wobble are compensated for both evaluations using all measuring fields.

The measurement conditions and the measurement grid for the structure-based macrolead analysis were developed in an extensive empirical measurement analysis as part of the FVA project FVA 876 I „3D-Macrolead“. Detailed and further information can be found in the final report [22].

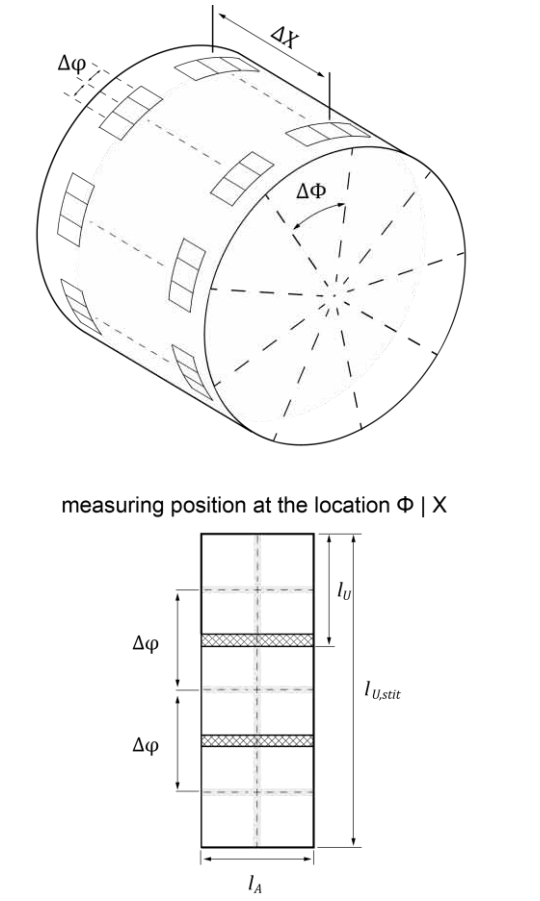

Figure 12: Recommended measurement grid for structure-based macrolead analysis

Table 6: Measurement conditions for structure-based macrolead analysis

Measurement method	optical
Lateral resolution	< 1.5 µm
Vertical resolution	< 10 nm

Table 7: Measurement grid for structure-based macrolead analysis

Number of circumferential positions	9
Distance between circ. measuring positions	ΔΦ = 40°
Number of axial positions	2
Distance between axial positions	ΔX = 4 mm
Number of overlapping measuring fields per position due to rotation	3
Distance between. the measuring fields per position[1]	$\Delta\varphi = \frac{360°}{\pi \cdot d} \cdot 0.85 \cdot l_U$
Measuring field size in axial direction	$l_A \geq 1.00$ mm
Measuring field size in circ. direction	$l_U \geq 1.15$ mm
Stitched topography length in circ. direction	$l_{U,stit} \geq 3.00$ mm

[1] The distance in the circumferential direction Δφ between the stitching measuring fields depends on the diameter of the shaft *d*, the measuring field size in the circumferential direction l_U and a defined overlap area.

A.2.2. Report Examples for Structure-Based Macrolead Analysis

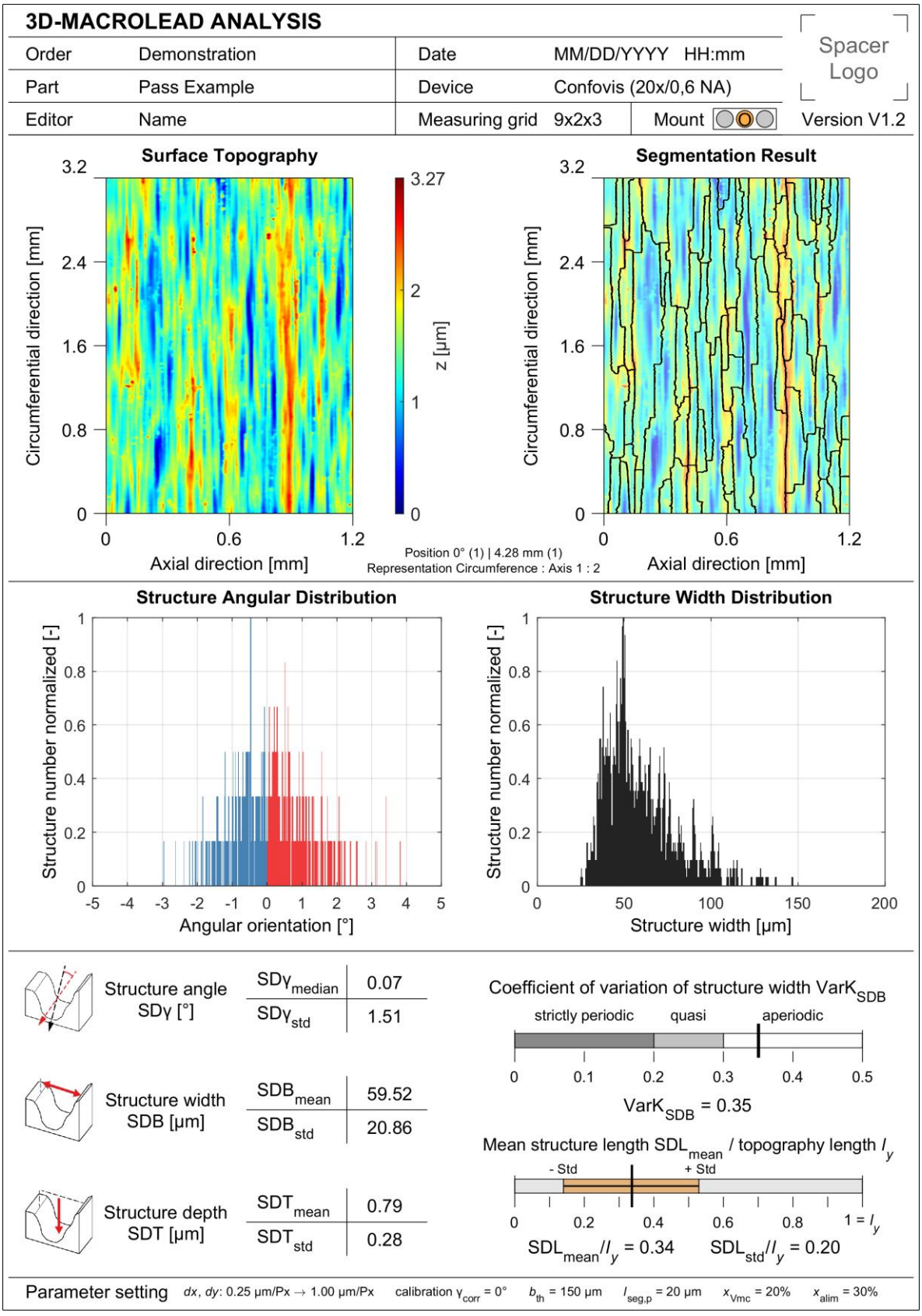

Figure 13: Report of the structure-based macrolead analysis of a pass example

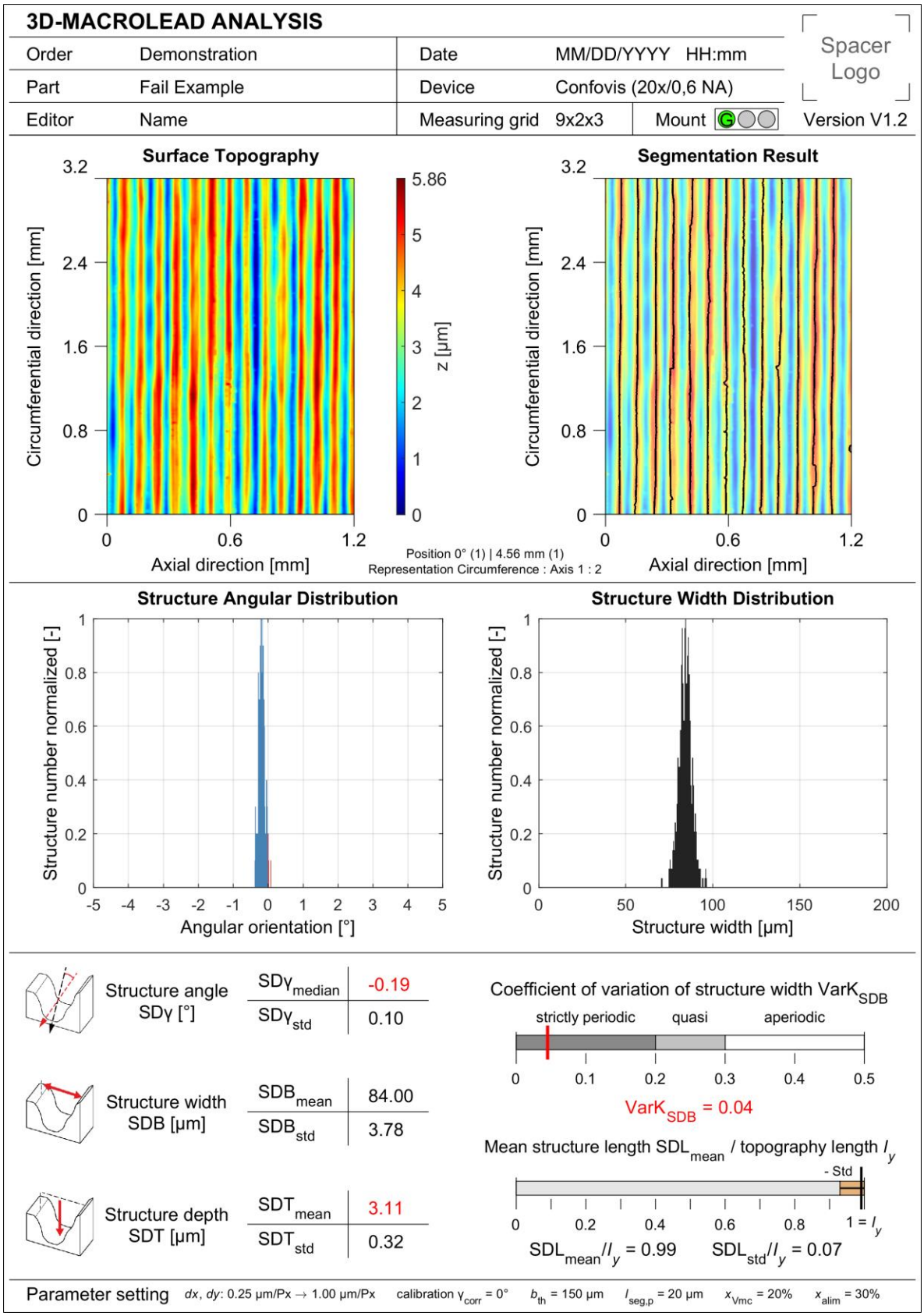

Figure 14: Report of the structure-based macrolead analysis of a fail example with periodic macrolead (small distribution width of the structure width distribution)

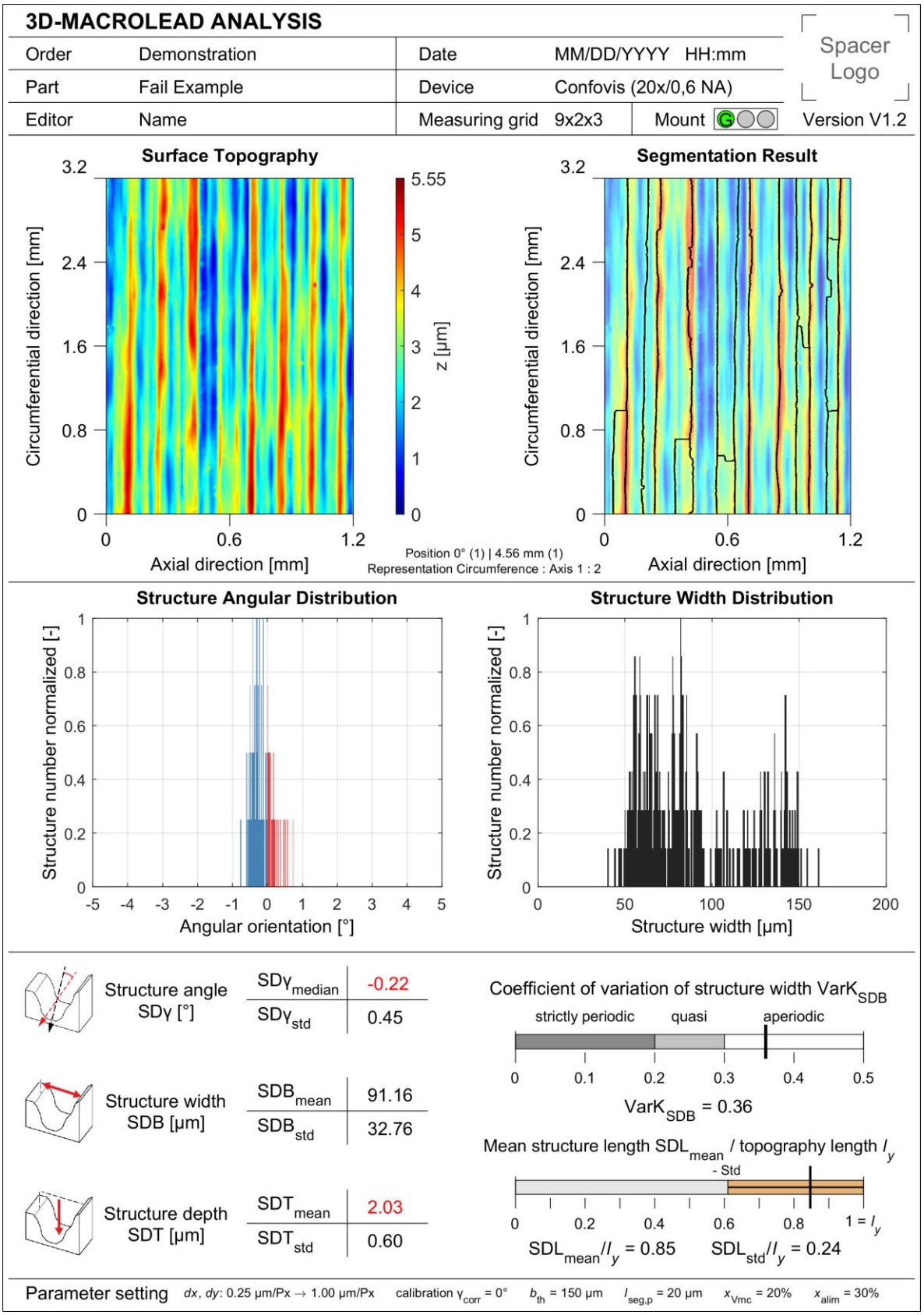

Figure 15: Report of the structure-based macrolead analysis of a fail example with aperiodic macrolead (large distribution width or several accumulation points in the structure width distribution)

A.3. Annex for Combined Structure-based Lead Analysis

A.3.1. Measurement Strategy for Combined Structure-based Lead Analysis

The measurement for the combined structure-based lead analysis includes the application of both the structure-based microlead analysis and the structure-based macrolead analysis to a single data set. This approach allows for the analysis of microlead as well as periodic and aperiodic macrolead through a single measurement process and evaluation. All results are presented in an overall "lead" report.

A measurement grid for the detection of microlead and periodic and aperiodic macrolead on the seal countersurface combines the measurement strategies of the structure-based microlead analysis (see Annex A.1) and the structure-based macrolead analysis (see Annex A.2). The following criteria must be met:

1) For a statistically reliable statement, the measuring fields must contain a sufficient number of microscopic grinding grooves. The number depends on the measuring field size and the number of measuring fields.

3) For a statistically reliable statement, the measuring fields must contain a sufficient number of macroscopic grinding structures. The number depends on the measuring field size and the number of measuring fields.

4) The surface topographies must be of sufficient length in the circumferential direction in order to enable an accurate assessment of the course of the structures and their orientation.

5) In order to detect and compensate for angular errors due to a misalignment of the shaft, multiple measurements in the axial and circumferential directions are necessary (wobble compensation).

To meet these criteria, it is recommended to measure the seal countersurface with a 9x2x3 measurement grid consisting of nine measurement positions in the circumferential direction at intervals of $\Delta\Phi = 40°$ at two axial positions at intervals of $\Delta X = 4$ mm. At each measurement position, three circumferentially overlapping measuring fields are recorded. The stitching of individual measuring fields with the instrument's own stitching function can be employed to achieve the required measuring field size.

These overlapping measurements are combined into a stitched topography for each measurement position within the structure-based macrolead analysis and evaluated as such. For the structure-based microlead analysis, one measuring field per measurement position is sufficient to achieve statistically accurate results. The angular misalignments of the shaft due to wobble are compensated for both evaluations using all measuring fields.

The measurement conditions and the measurement grid for the combined structure-based lead analysis were developed as part of the FVA project FVA 975 I "FVA Guideline Surface/Lead – Shaft Seals."

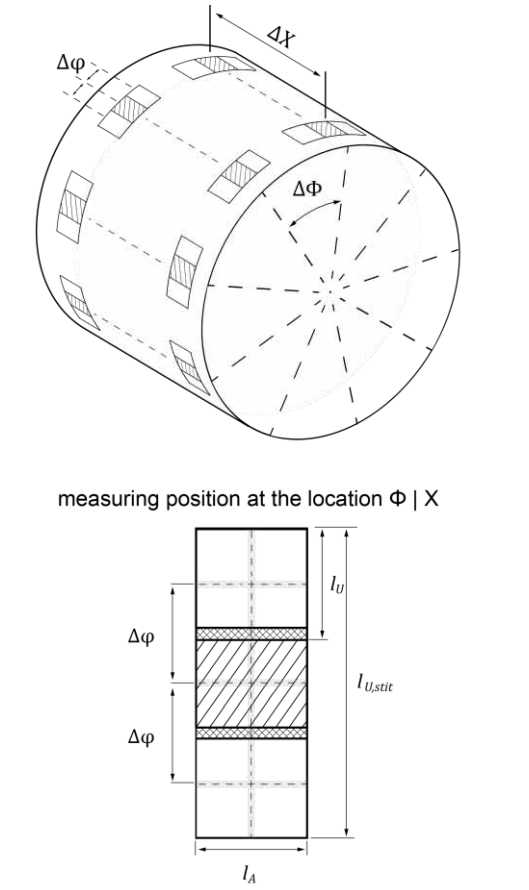

Figure 16: Recommended measurement grid for combined structure-based lead analysis

Table 8: Measurement conditions for structure-based lead analysis

Measurement method	optical
Lateral resolution	< 1.5 µm
Vertical resolution	< 10 nm

Table 9: Recommended measurement grid for combined structure-based lead analysis

Number of circumferential positions	9
Distance between circ. measuring positions	ΔΦ = 40°
Number of axial positions	2
Distance between axial positions	ΔX = 4 mm
Number of overlapping measuring fields per position due to rotation	3
Distance between. the measuring fields per position[1]	$\Delta\varphi = \frac{360°}{\pi \cdot d} \cdot 0.85 \cdot l_U$
Measuring field size in axial direction	l_A ≥ 1.00 mm
Measuring field size in circ. direction	l_U ≥ 1.15 mm
Stitched topography length in circ. direction	$l_{U,stit}$ ≥ 3.00 mm

[1] The distance in the circumferential direction Δφ between the stitching measuring fields depends on the diameter of the shaft *d*, the measuring field size in the circumferential direction l_U and a defined overlap area.

A.3.2. Report Examples for Combined Structure-Based Lead Analysis

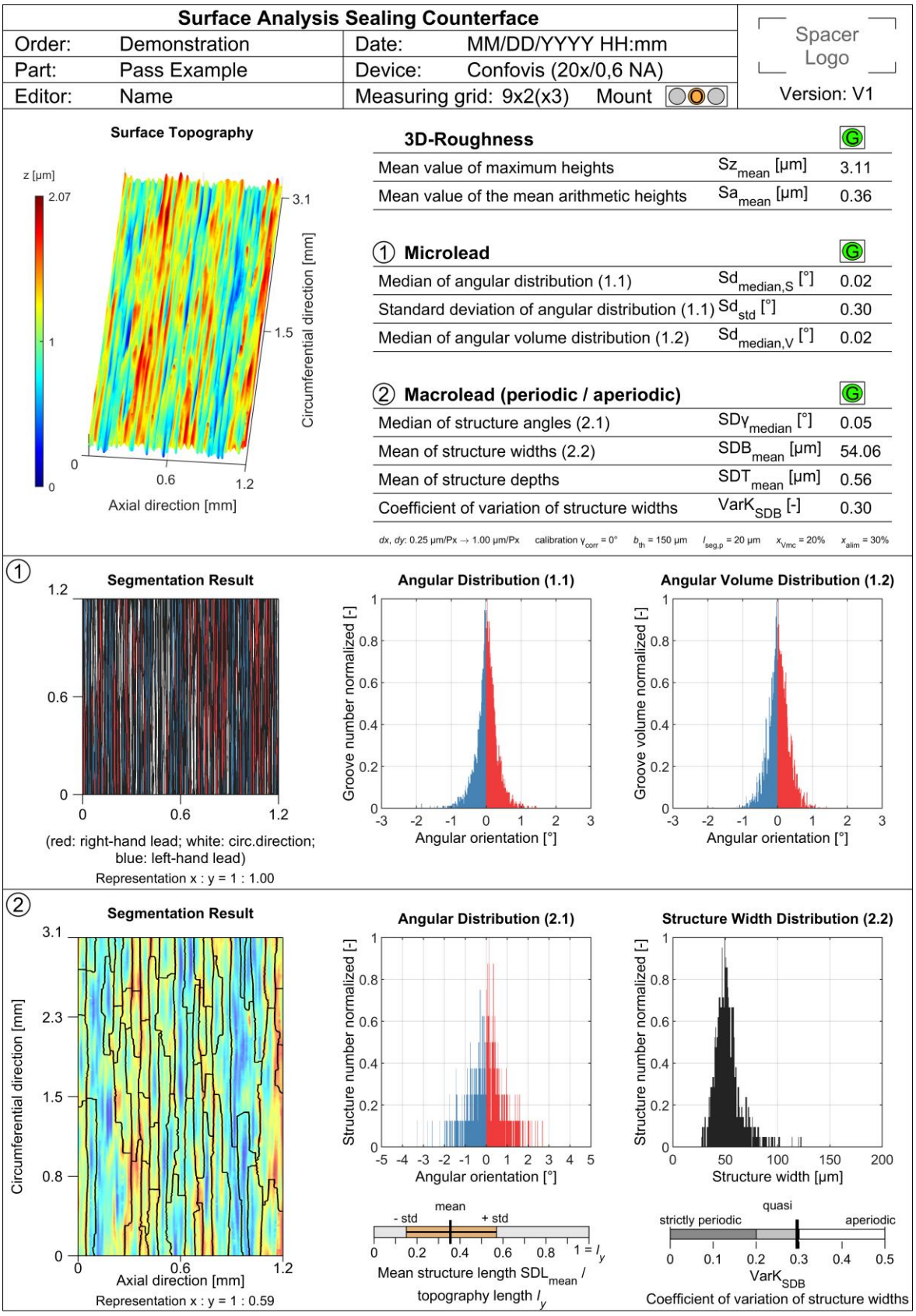

Figure 17: Overall "lead" report of a pass example

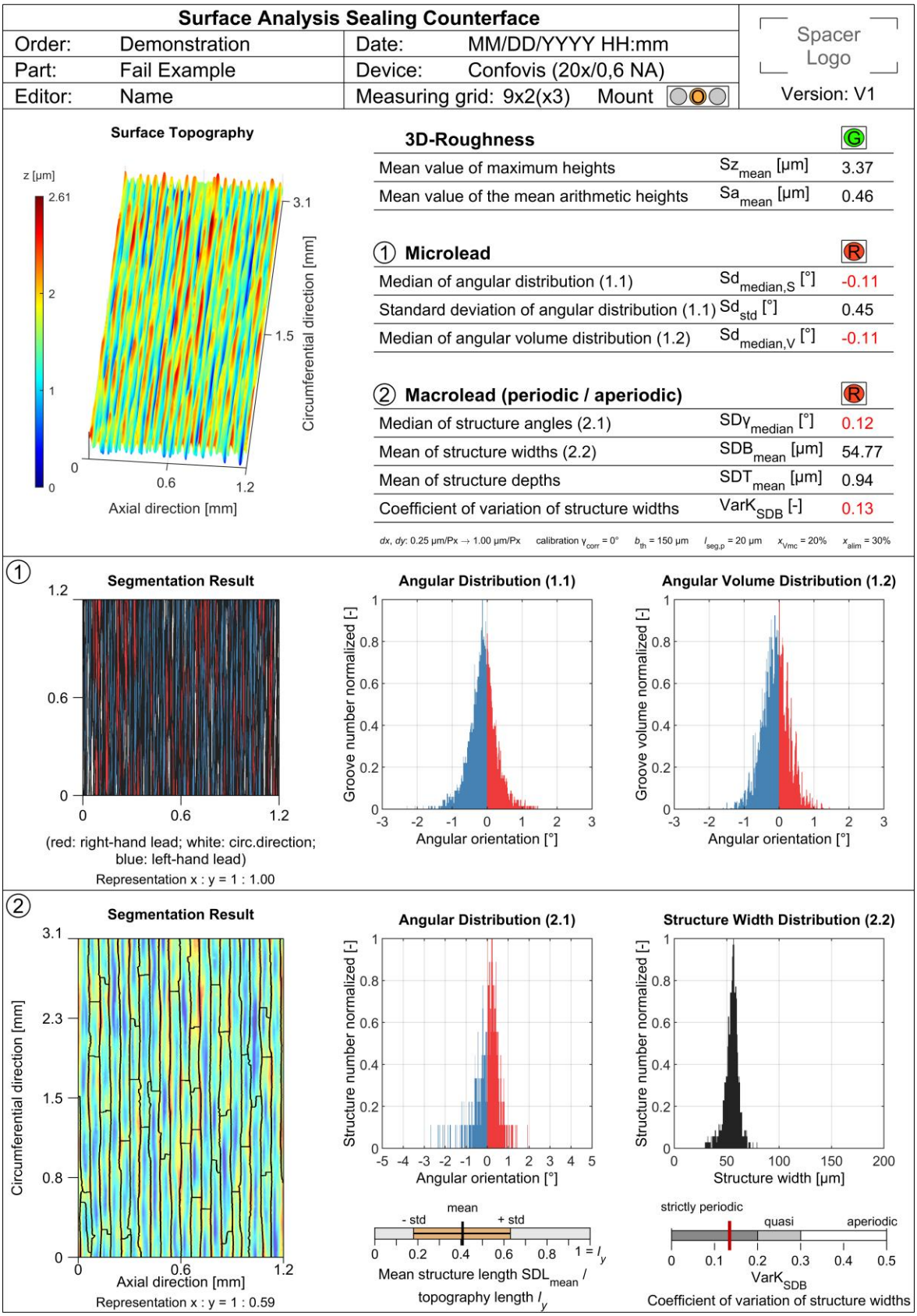

Figure 18: Overall "lead" report of a fail example

A.4. Annex for Macrolead Evaluation according to MBN 31007-7

A.4.1. Measurement Strategy for Macrolead Evaluation according to MBN 31007-7

The measurement is based on axial-parallel surface profiles, which are measured 72 times in a 360° measurement grid in 5° steps and in a 36° measurement grid in 0.5° steps (see Figure 19). The parameters of the measurement grids are summarized in Table 10.

The 72 individual profiles are combined into a topography representation. A frequency analysis (FFT) is used to identify and mathematically approximate periodic macrolead. From the mathematical approximation, the macrolead parameters according to MBN 31007-7 can be determined, as illustrated in Figure 20.

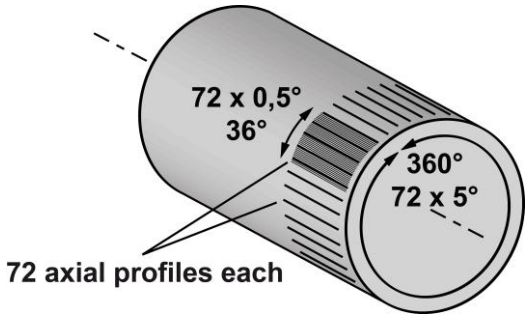

Figure 19: Macrolead Evaluation according to MBN 31007-7

Table 10: Measurement grid for macro-lead evaluation according to MBN 31007-

Profile measurements per grid (360°/36°)	72
Axial measurement length	2 mm
Step size in circumferential direction for 360° measurement	5°
Step size in circumferential direction for 36° measurement	0.5°

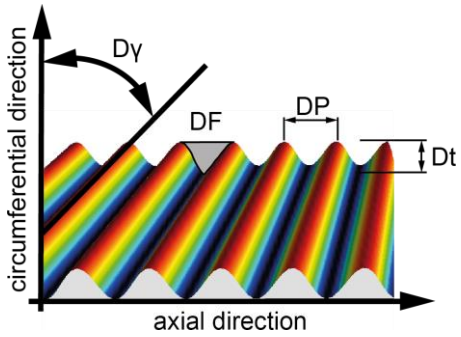

Dγ	Lead Angle
DP	Period Length
Dt	Lead Depth
DF	Theoretical Supply Cross Section

Figure 20: Mathematically approximated surface and lead parameters according to MBN 31007-7

A.4.2. Report Examples for or Macrolead Evaluation according to MBN 31007-7

Identity card - Pass 360°	
Name:	Pass 360°
NM-points ratio:	0.00 % (0 Pts)

Sapcer Logo

Parameters		Value	Unit	Parameters		Value	Unit
Diameter		50.0	mm	Period length	DP	0.274	mm
Evaluation length		2.00	mm	Theoretical supply cross section	DF	19.5	µm²
Maximum wavelength		0.400	mm	Theoretical supply cross section per turn	DFu	0.00	µm²/U
Number of threads	DG	0.00		Contact length in percent	DLu	100	%
Lead depth	Dt	0.141	µm	Lead angle	Dγ	0.00	°

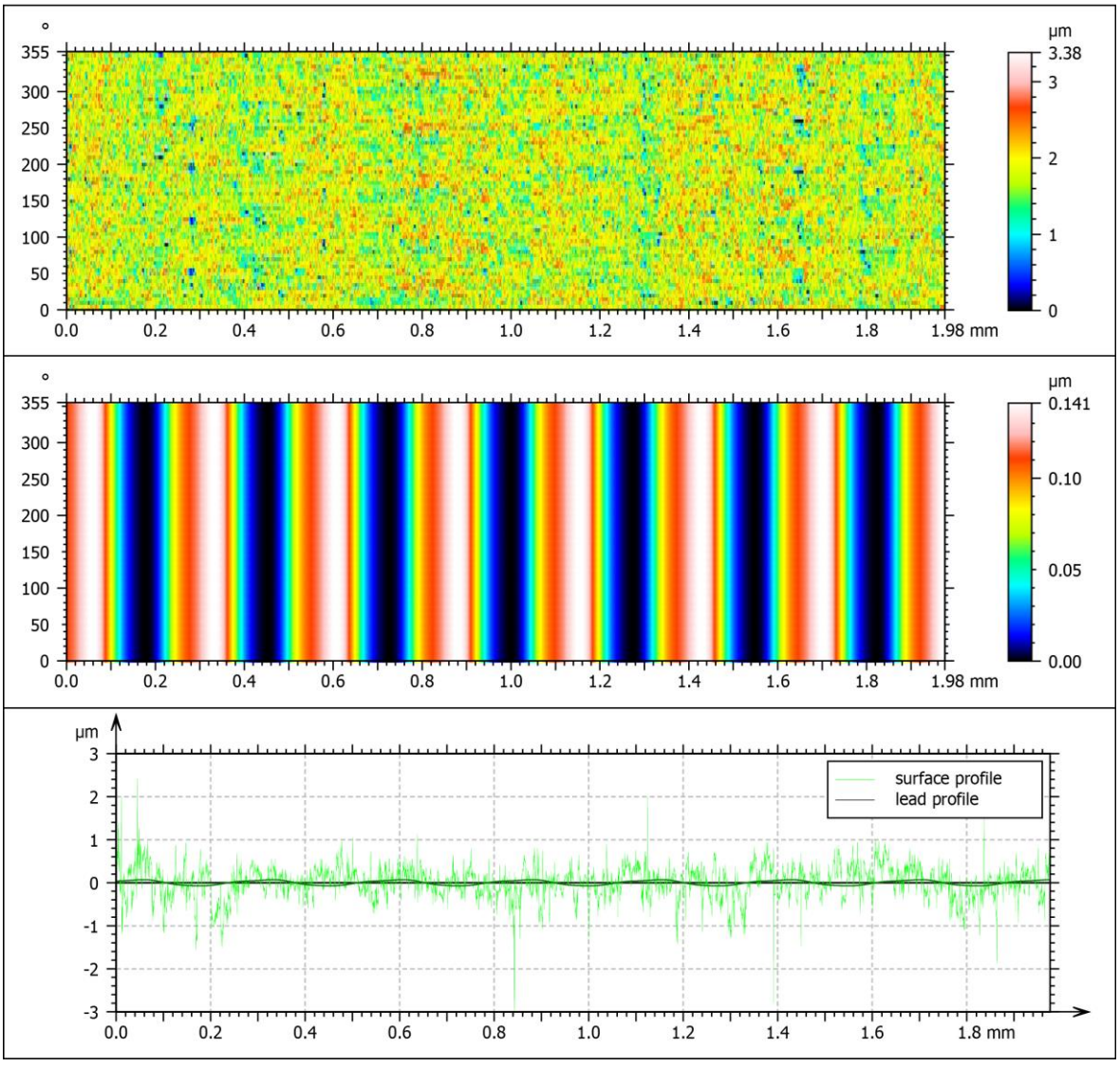

Figure 21: Report of the 360° macrolead evaluation according to MBN 31007-7 of a pass example (evaluated with HommelMap Premium Version 7.4.9745 2021/06/06)

Identity card - Pass 360°	
Name:	Pass 360°
NM-points ratio:	0.00 % (0 Pts)

Sapcer Logo

Parameters		Value	Unit	Parameters		Value	Unit
Diameter		50.0	mm	Period length	DP	0.274	mm
Evaluation length		2.00	mm	Theoretical supply cross section	DF	21.3	µm²
Maximum wavelength		0.400	mm	Theoretical supply cross section per turn Irehung	DFu	0.00	µm²/U
Number of threads	DG	0.00		Contact length in percent	DLu	100	%
Lead depth	Dt	0.153	µm	Lead angle	Dγ	0.00	°

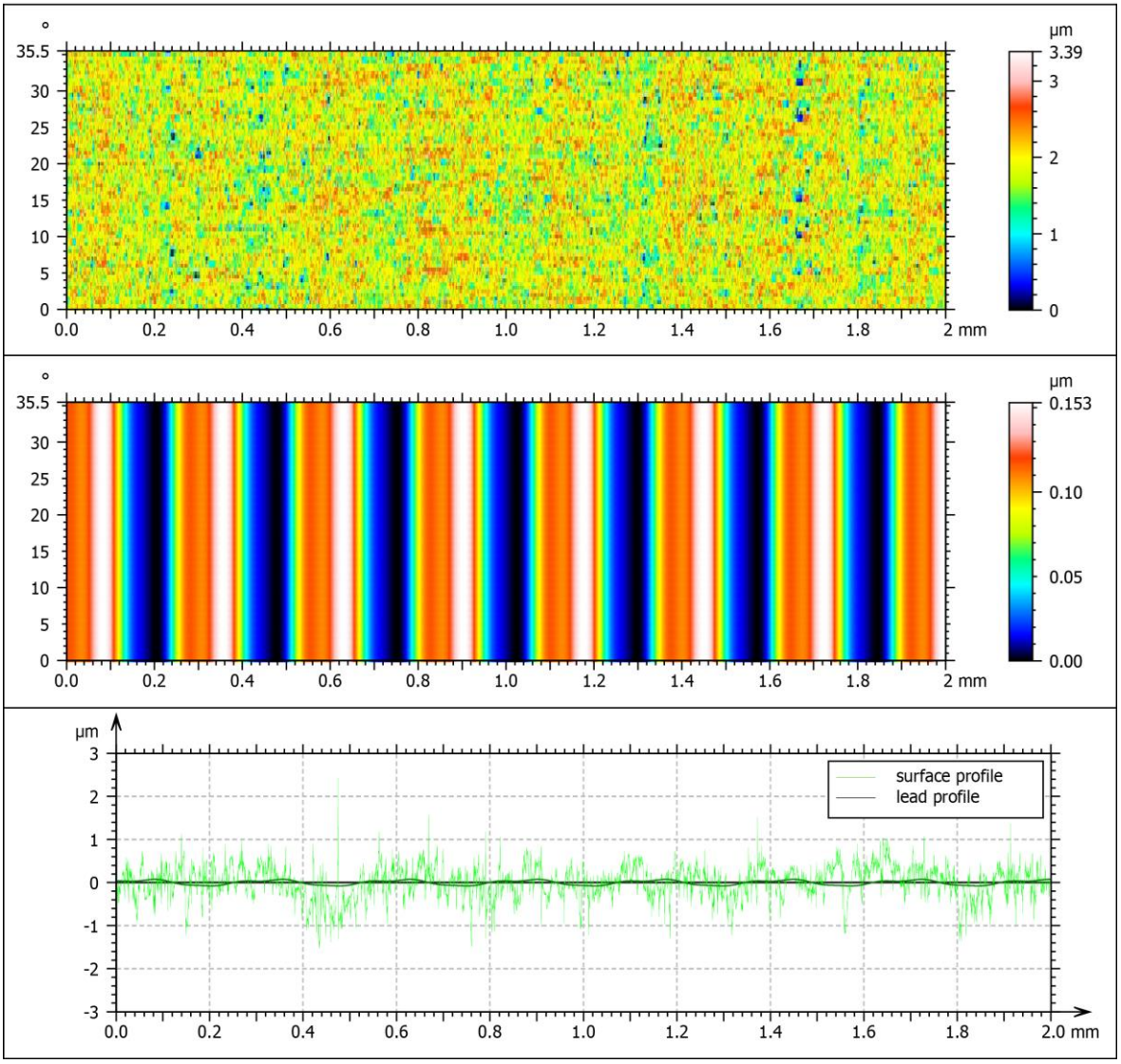

Figure 22: Report of the 36° macrolead evaluation according to MBN 31007-7 of a pass example (evaluated with HommelMap Premium Version 7.4.9745 2021/06/06)

Identity card - Fail 360°	
Name:	Fail 360°
NM-points ratio:	0.00 % (0 Pts)

Sapcer Logo

Parameters		Value	Unit	Parameters		Value	Unit
Diameter		50.0	mm	Period length	DP	0.135	mm
Evaluation length		2.00	mm	Theoretical supply cross section	DF	106	µm²
Maximum wavelength		0.400	mm	Theoretical supply cross section per turn	DFu	1059	µm²/U
Number of threads	DG	10.0		Contact length in percent	DLu	22.9	%
Lead depth	Dt	1.44	µm	Lead angle	Dγ	0.492	°

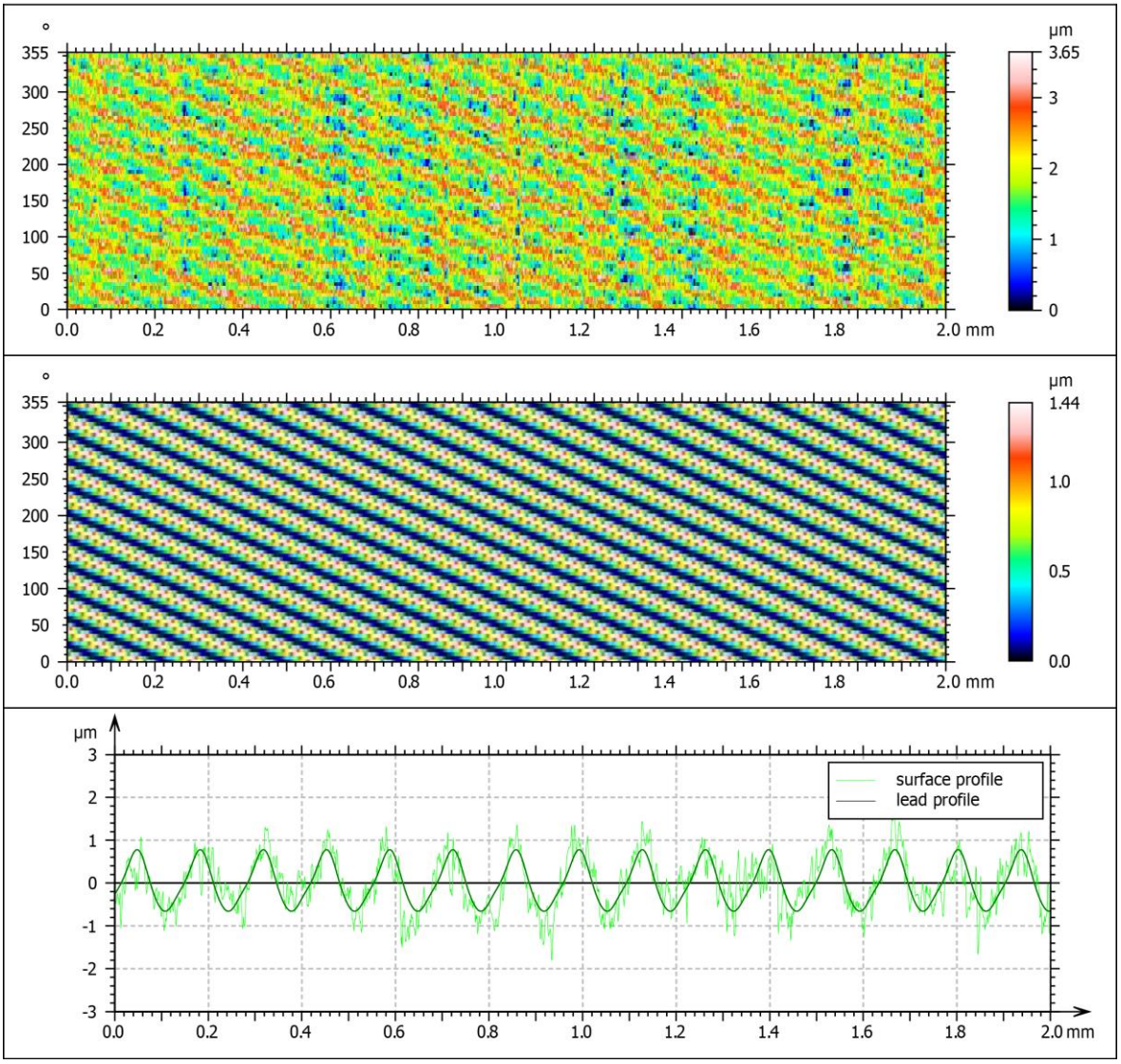

Figure 23: Report of the 360° macrolead evaluation according to MBN 31007-7 of a fail example with periodic macrolead (evaluated with HommelMap Premium Version 7.4.9745 2021/06/06)

Identity card - Fail 36°	
Name:	Fail 36°
NM-points ratio:	0.00 % (0 Pts)

Sapcer Logo

Parameters		Value	Unit	Parameters		Value	Unit
Diameter		50.0	mm	Period length	DP	0.135	mm
Evaluation length		2.00	mm	Theoretical supply cross section	DF	105	µm²
Maximum wavelength		0.400	mm	Theoretical supply cross section per turn	DFu	1046	µm²/U
Number of threads	DG	10.0		Contact length in percent	DLu	22.1	%
Lead depth	Dt	1.41	µm	Lead angle	Dγ	0.492	°

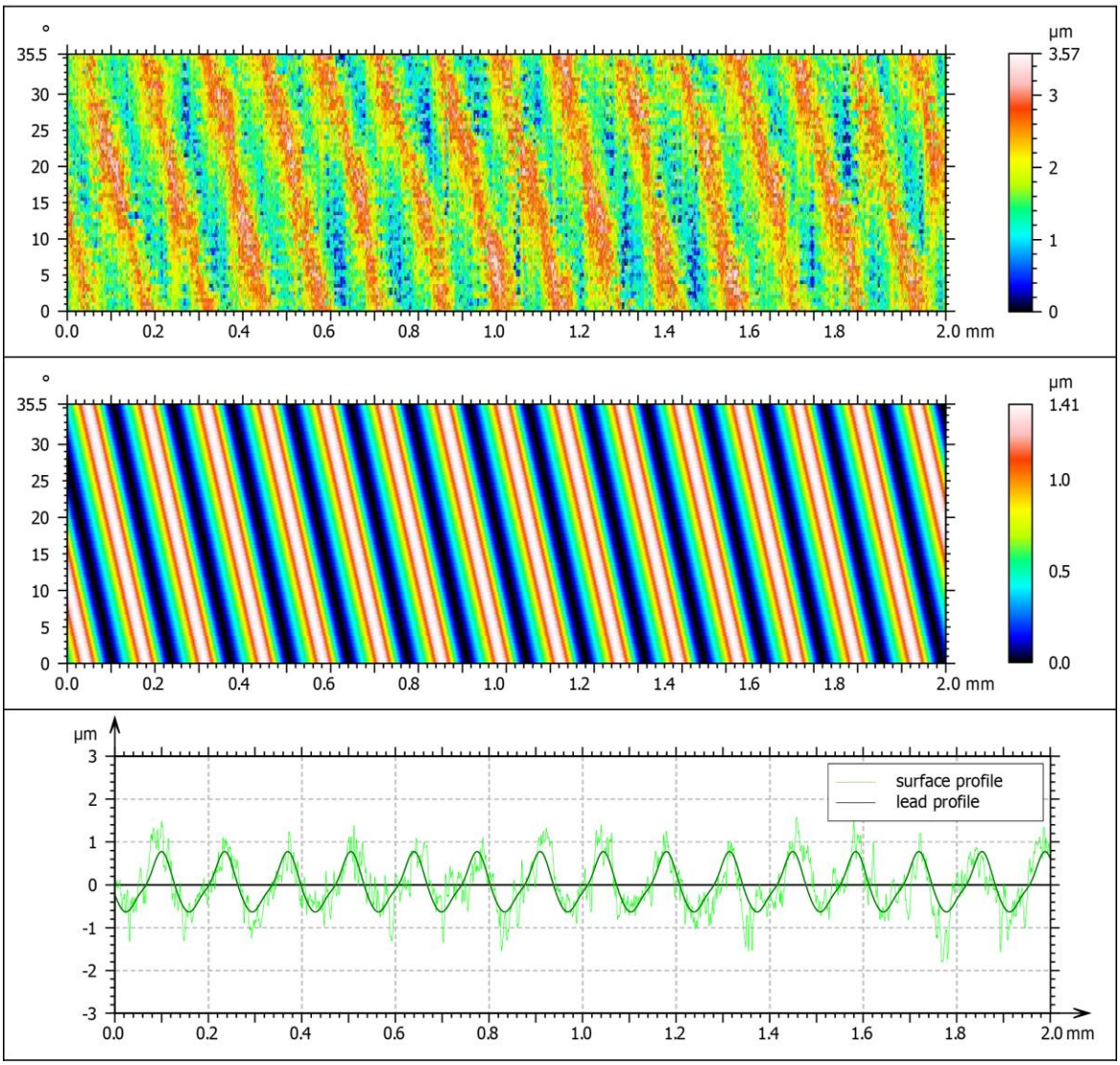

Figure 24: Report of the 36° macrolead evaluation according to MBN 31007-7 of a fail example with periodic macrolead (evaluated with HommelMap Premium Version 7.4.9745 2021/06/06)

A.5. Annex for Lead Testing using the Thread Method

There is no generally accepted standardization for the thread method. Various guidelines and company standards exist, specifying different threads, speeds, and weights. In this FVA guideline, the following specifications are recommended:

Table 11: Recommended specifications for the thread method

Thread type	Cotton thread Mercifil 40
Shaft surface	Dry
Duration	10 s per rotation direction
Rotation speed	60 rpm
Weight	35 g
Wrapping angle thread - shaft:	220 – 240°

Note: Particularly with larger shaft diameters, both the thread and the attached weight may be carried in the circumferential direction. It is recommended to increase the weight in this case.

The schematic configuration of the lead testing with the thread method is illustrated in Figure 25. Figure 26 shows an example of an enlarged image of the thread on the shaft surface.

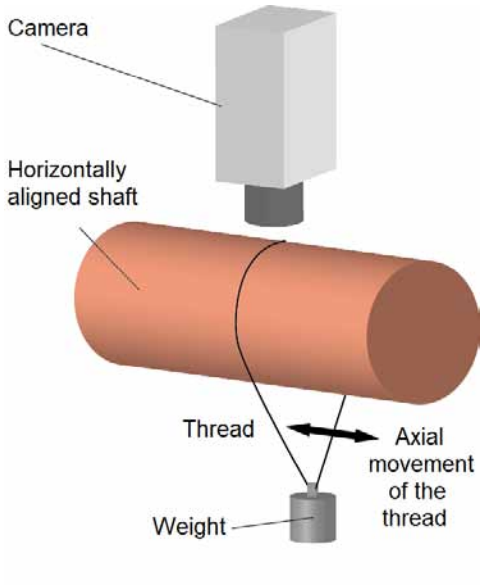

Figure 25: Schematic configuration of the lead testing with the thread method

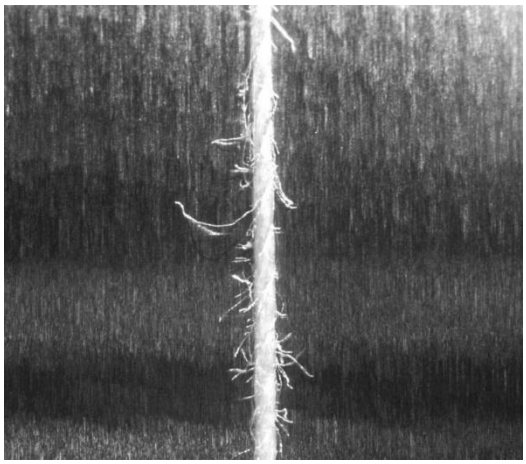

Figure 26: Thread on the shaft surface